Available online at www.sciencedirect.com
ScienceDirect
Journal of Computational Physics 227 (2007) 983–1006
JOURNAL OF COMPUTATIONAL PHYSICS
www.elsevier.com/locate/jcp

A posteriori error estimation and basis adaptivity for reduced-basis approximation of nonaffine-parametrized linear elliptic partial differential equations

N.C. Nguyen *

Department of Aeronautics and Astronautics, Massachusetts Institute of Technology, Rm 37-435, 77 Massachusetts Avenue, Cambridge, MA 02139, USA

Received 16 March 2007; received in revised form 21 July 2007; accepted 21 August 2007
Available online 14 September 2007

Abstract

In this paper, we extend the earlier work [M. Barrault, Y. Maday, N. C. Nguyen, A.T. Patera, An "empirical interpolation" method: application to efficient reduced-basis discretization of partial differential equations, C.R. Acad. Sci. Paris, Série I 339 (2004) 667–672; M.A. Grepl, Y. Maday, N.C. Nguyen, A.T. Patera, Efficient reduced-basis treatment of nonaffine and nonlinear partial differential equations, M2AN Math. Model. Numer. Anal. 41 (3) (2007) 575–605.] to provide *a posteriori* error estimation and basis adaptivity for reduced-basis approximation of linear elliptic partial differential equations with *nonaffine* parameter dependence. The essential components are (i) rapidly convergent reduced-basis approximations – (Galerkin) projection onto a space W_N^u spanned by N global hierarchical basis functions which are constructed from solutions of the governing partial differential equation at judiciously selected points in parameter space; (ii) stable and inexpensive interpolation procedures – methods which allow us to replace nonaffine parameter functions with a coefficient-function expansion as a sum of M products of parameter-dependent coefficients and parameter-independent functions; (iii) *a posteriori* error estimation – relaxations of the error-residual equation that provide inexpensive yet sharp error bounds for the error in the outputs of interest; (iv) optimal basis construction – processes which make use of the error bounds as an inexpensive surrogate for the expensive true error to explore the parameter space in the quest for an optimal sampling set; and (v) offline/online computational procedures – methods which decouple the generation and projection stages of the approximation process. The operation count for the online stage – in which, given a new parameter value, we calculate the output of interest and associated error bounds – depends only on N, M, and the affine parametric complexity of the problem; the method is thus ideally suited for repeated and reliable evaluation of input–output relationships in the many-query or real-time contexts.
Published by Elsevier Inc.

Keywords: Nonaffine-parametrized partial differential equations; Reduced basis methods; Galerkin approximation; Coefficient-function approximation; Output bounds; *A posteriori* error estimation; Basis adaptivity

* Tel.: +1 617 253 8080.
E-mail address: cuongng@mit.edu

0021-9991/$ - see front matter Published by Elsevier Inc.
doi:10.1016/j.jcp.2007.08.031

1. Introduction

The design and optimization of engineering systems often requires repeated, reliable, and real-time prediction of an (or more realistically, several) "output of interest" $s^e \in \mathbb{R}$-related to maximum displacements, critical stresses or strains, energies or forces, flowrates or pressure drops, temperatures or fluxes – as a function of an "input" parameter P-vector $\mu \in \mathcal{D} \subset \mathbb{R}^P$-related to geometry, physical properties, boundary conditions, or loads. These outputs are often functionals of a field variable $u^e(\mu)$,

$$s^e(\mu) = \ell(u^e(\mu)), \tag{1}$$

where $u^e(\mu) \in X^e$ – say displacement, velocity, or temperature – satisfies the weak form of the μ-parametrized elliptic partial differential equation (PDE)

$$a(u^e(\mu), v; \mu) = f(v), \quad \forall v \in X^e. \tag{2}$$

Here X^e is the appropriate function space, and a (respectively ℓ, f) are continuous bilinear (respectively, linear) forms. The relevant system behavior is thus described by an implicit input–output relationship, $\mu \to s^e(\mu)$, evaluation of which demands solution of the underlying PDE.

In general, we cannot find the exact solution, and hence we replace $s^e(\mu)$, $u^e(\mu)$ with a Galerkin finite element approximation, $s^{\mathcal{N}}(\mu), u^{\mathcal{N}}(\mu)$: given $\mu \in \mathcal{D}$,

$$s^{\mathcal{N}}(\mu) = \ell(u^{\mathcal{N}}(\mu)), \tag{3}$$

where $u^{\mathcal{N}}(\mu) \in X^{\mathcal{N}}$ satisfies

$$a(u^{\mathcal{N}}(\mu), v; \mu) = f(v), \quad \forall v \in X^{\mathcal{N}}. \tag{4}$$

Here $X^{\mathcal{N}} \subset X^e$ is a standard finite element approximation subspace of dimension $\mathcal{N}$. Unfortunately, to achieve the desired accuracy, $\mathcal{N}$ must typically be chosen very large; as a result, the evaluation $\mu \to s^{\mathcal{N}}(\mu)$ is simply too costly in the many-query and real-time contexts often of interest in engineering.

For parametrized PDEs, the fundamental observation is that $u^{\mathcal{N}}(\mu)$ in fact resides on a very low-dimensional manifold $\mathcal{M}^u = \{u^{\mathcal{N}}(\mu), \mu \in \mathcal{D}\}$ induced by the parametric dependence. Furthermore, the field variable $u^{\mathcal{N}}(\mu)$ will often be quite regular in μ – the parametrically induced manifold $\mathcal{M}^u$ is smooth – even when the field variable enjoys only limited regularity with respect to the spatial coordinate. The reduced-basis (RB) method explicitly recognizes and exploits dimension reduction afforded by the low-dimensional smooth solution manifold to develop RB approximations of $u^{\mathcal{N}}(\mu)$, $s^{\mathcal{N}}(\mu)$.

In the RB method, we first require a space W_N^u spanned by N global basis functions ζ_n, $1 \leqslant n \leqslant N$; here the dimension N is very small compared to $\mathcal{N}$. Typically, these basis functions are constructed from a "snapshot set" which consists of solutions of the underlying PDE at selected parameter points. We next seek an approximation $u_N(\mu) \in W_N^u$ by applying a Galerkin projection

$$a(u_N(\mu), v; \mu) = f(v), \quad \forall v \in W_N^u. \tag{5}$$

We then substitute $u_N(\mu) = \sum_{j=1}^N \underline{u}_{Nj}(\mu)\zeta_j$ and choose $v = \zeta_i$, $1 \leqslant i \leqslant N$, to obtain

$$\underline{A}_N(\mu)\underline{u}_N(\mu) = \underline{F}_N, \tag{6}$$

where $\underline{A}_N(\mu) \in \mathbb{R}^{N\times N}$, $\underline{F}_N \in \mathbb{R}^N$ are the RB stiffness matrix and force vector with entries $\underline{A}_{N\,ij}(\mu) = a(\zeta_j, \zeta_i; \mu)$, $\underline{F}_{N\,i} = f(\zeta_i)$, $1 \leqslant i,j \leqslant N$, respectively. Once solving for $\underline{u}_N(\mu)$, we evaluate the RB approximation $s_N(\mu)$ to $s^{\mathcal{N}}(\mu)$ as

$$s_N(\mu) = \ell(u_N(\mu)) = \sum_{j=1}^N \underline{u}_{Nj}(\mu)\underline{L}_{Nj}. \tag{7}$$

Here $\underline{L}_N \in \mathbb{R}^N$ is the RB output vector with entries $\underline{L}_{N\,i} = \ell(\zeta_i)$, $1 \leqslant i \leqslant N$. We note that the (full) RB system (6) of size $N \times N$ is very small compared to the (sparse) $\mathcal{N} \times \mathcal{N}$ linear system associated with the finite element discretization (4). Since $N \ll \mathcal{N}$, the RB method can effect a significant reduction in the degrees of freedom. Nevertheless, the RB system (6) can still be expensive as the operation count of assembling the stiffness matrix $a(\zeta_j, \zeta_i; \mu)$ depends on $\mathcal{N}$.

In the literature, RB methods [3–10] and associated *a posteriori* error estimation procedures [7,11–17] have been developed for linear elliptic PDEs with *affine* parameter dependence, in particular, problems which accept an affine decomposition hypothesis: for some finite (preferably small) integer Q, a may be expressed as

$$a(w,v;\mu)=\sum_{q=1}^{Q}\Theta^q(\mu)a^q(w,v),\quad \forall w,v\in X,\quad \forall \mu\in\mathcal{D}, \tag{8}$$

where $\Theta^q:\mathcal{D}\to\mathbb{R}$ and $a^q(w,v):X\times X\to\mathbb{R}$, $1\leqslant q\leqslant Q$, are parameter-dependent functions and parameter-independent continuous bilinear forms, respectively. Under the above hypothesis, we can write

$$\underline{A}_N(\mu)=\sum_{q=1}^{Q}\Theta^q(\mu)\underline{A}_N^q, \tag{9}$$

where, for $1\leqslant q\leqslant Q$, the matrices $\underline{A}_N^q\in\mathbb{R}^{N\times N}$ with entries $a^q(\zeta_j,\zeta_i)$ are *parameter-independent* and can thus be pre-computed offline. Hence, in the online stage, forming $\underline{A}_{\mathcal{N}}(\mu)$ according to (9) and inverting it require only $O(QN^2+N^3)$ operations. The online complexity is totally *independent* of $\mathcal{N}$. The traditional RB approach proves very effective for affine parameter problems.

Unfortunately, if a is not affine in the parameter this computational strategy breaks down; the online complexity will still depend on $\mathcal{N}$. For example, for *general* functions $g^r(x;\mu)$, $1\leqslant r\leqslant R$, (here $x\in\Omega$ and $\mu\in\mathcal{D}$), the bilinear form

$$a(w,v;\mu)=\sum_{r=1}^{R}c^r(w,v,g^r(x;\mu)) \tag{10}$$

will not admit an efficient (online $\mathcal{N}$-independent) computational decomposition. Here $c^r:X\times X\times L^\infty(\Omega)\to\mathbb{R}$ are trilinear forms. It is obvious that (9) is merely a special case of (10) in which $Q=R$, $g^r(x;\mu)=\Theta^r(\mu)$, and $c^r(w,v,g^r(x;\mu))$ reduces to $\Theta^r(\mu)a^r(w,v)$ for $1\leqslant r\leqslant R$ – $g^r(\cdot;\mu)$ depends only on the parameter μ, *not* on the spatial coordinates x. Although many property, boundary condition, load, and even geometry variations can indeed be expressed in the affine hypothesis (9) for reasonably small Q, there are many problems – for example, geometric variations considered in this paper – which do not admit such a decomposition, but the more general nonaffine representation (10).

Indeed, the limitation of the affine decomposition hypothesis prompts the development of efficient RB approaches for nonaffine-parametrized PDEs. In [1,2], the authors introduce the empirical interpolation method and apply the method to replace nonaffine-parametrized functions with a coefficient-function approximation which recovers $\mathcal{N}$-independent complexity for the online computation. The RB technique developed therein has been applied not only to nonaffine linear elliptic equations but also to highly nonlinear elliptic and parabolic equations [2], as well as certain nonlinear problems in quantum chemistry [18]. The effective treatment of nonaffine terms by the empirical interpolation approach results in a low order model which is typically several orders of magnitude less expensive than the high-fidelity finite element model (4) and standard Galerkin reduced-order model built upon (5).

For parametrized PDEs with affine parameter dependence, *a posteriori* error estimation procedures have been developed for linear elliptic and parabolic problems [7,11–13,17,19] and for nonlinear problems including the incompressible Navier–Stokes equations [14–16,20]. However, in the case of nonaffine parameter dependence, the development of *a posteriori* error estimators is not totally straightforward. Another important issue is the construction of a reduced basis $\{\zeta_n\}_{n=1}^N$. For many low-order methods, the reduced basis is constructed upon a snapshot set consisting of finite element solutions of the underlying PDE at selected parameter points. It is thus very important to find a small yet optimal set of parameter points by which we compute the snapshots and construct our reduced basis.

In this paper we shall expand upon the earlier work [1,2] to provide *a posteriori* error estimation and basis adaptivity for the RB approximation of linear elliptic PDEs with nonaffine parameter dependence. The new contributions are the *a priori* convergence analysis, the derivation of *a posteriori* error estimators, and the optimal construction of hierarchical RB spaces based on the greedy sampling procedure [16,20,19] and proper orthogonal decomposition (POD) or Karhunen–Loève (KL) approach [21–23].

This paper is organized as follows. In Section 2, we introduce the problem statement. In Section 3, we present a short review of the empirical interpolation method. In Section 4, we discuss the RB approximation and computational considerations. In Section 5, we develop the associated *a posteriori* error estimation procedure to obtain error bounds for the field variable and output of interest. In Section 6, we describe the basis adaptivity procedure to generate optimal RB spaces. In Section 7, we present numerical results for a heat conduction problem in a parametrized domain in view of the engineering design of a heat shield configuration. Finally, in Section 8, we conclude the paper with some remarks.

2. Problem statement

2.1. Preliminaries

We shall consider second-order elliptic PDEs, and hence our exact space X^e satisfies $H_0^1(\Omega) \subset X^e \subset H^1(\Omega)$. Here $\Omega \subset \mathbb{R}^d$ ($d = 1$, 2, or 3) is a spatial domain with suitably regular boundary $\partial\Omega$; $H^1(\Omega) = \{v \in L^2(\Omega), \nabla v \in (L^2(\Omega))^d\}$; and $L^2(\Omega)$ is the space of square integrable functions over Ω. The inner product and norm associated with X^e are given by $(\cdot,\cdot)_{X^e}$ and $\|\cdot\|_{X^e} = (\cdot,\cdot)_{X^e}^{1/2}$, respectively. A typical choice for our inner product $(\cdot,\cdot)_{X^e}$ is

$$(w, v)_{X^e} = \int_\Omega \nabla w \cdot \nabla v + wv, \quad \forall w, v \in X^e, \tag{11}$$

which is simply the standard $H^1(\Omega)$ inner product. Any inner product which induces a norm equivalent to the H^1 norm is acceptable.

We shall denote by X'^e the dual space of X^e. For a $h \in X'^e$, the dual norm is given by

$$\|h\|_{X'^e} \equiv \sup_{v \in X^e} \frac{h(v)}{\|v\|_{X^e}}. \tag{12}$$

If we introduce the representation operator $\mathcal{Y} : X'^e \to X^e$ such that, for any $h \in X'e$,

$$(\mathcal{Y}h, v)_{X^e} = h(v), \quad \forall v \in X^e, \tag{13}$$

then

$$\|h\|_{X'^e} = \|\mathcal{Y}h\|_{X^e}. \tag{14}$$

This is simply a statement of the Riesz representation theorem.

2.2. Problem formulation

Our exact output and field variable, $s^e(\mu) \in \mathbb{R}$ and $u^e(\mu) \in X^e$, satisfy (1) and (2). Here, for any $\mu \equiv (\mu^1 \cdots \mu^P)$ in our closed input domain $\mathcal{D} \subset \mathbb{R}^P$, $a(\cdot,\cdot;\mu) : X^e \times X^e \to \mathbb{R}$ is a parameter-dependent bilinear form, and $\ell(\cdot) : X^e \to \mathbb{R}$ and $f(\cdot) : X^e \to \mathbb{R}$ are parameter-independent linear forms.

Our "truth" or "reference" finite element approximation to the exact output and field variable, $s(\mu) \equiv s^{\mathcal{N}_t}(\mu)$ and $u(\mu) \equiv u^{\mathcal{N}_t}(\mu) \in X^{\mathcal{N}_t} \equiv X$, satisfies (3) and (4) for the particular choice $\mathcal{N} = \mathcal{N}_t$: given $\mu \in \mathcal{D}$, we find

$$s(\mu) = \ell(u(\mu)), \tag{15}$$

where $u(\mu) \in X$ satisfies

$$a(u(\mu), v; \mu) = f(v), \quad \forall v \in X. \tag{16}$$

We assume that $\mathcal{N}_t$ is chosen sufficiently large that $s(\mu)$ and $u(\mu)$ are essentially indistinguishable from $s^e(\mu)$ and $u^e(\mu)$, respectively. We shall build our reduced basis approximation upon this "truth" approximation; and we shall evaluate the error in our reduced basis approximation with respect to this "truth" approximation. As we will subsequently prove in Sections 4 and 5, the online complexity (and stability) of our reduced basis approach is *independent* of $\mathcal{N}_t$; hence, we may choose $\mathcal{N}_t$ to be "arbitrarily" large at *no detriment to (online) performance*.

In this paper, we shall consider a particular form for the operator a: for some fixed integer Q and R, a can be expressed as

$$a(w,v;\mu) = \sum_{q=1}^{Q} \Theta^q(\mu) b^q(w,v) + \sum_{r=1}^{R} c^r(w,v,g^r(x;\mu)) \tag{17}$$

for all $w, v \in X$ and for all $\mu \in \mathcal{D}$. Here $\Theta^q : \mathcal{D} \to \mathbb{R}$ and $b^q(w,v) : X \times X \to \mathbb{R}$, $1 \leqslant q \leqslant Q$, are μ-dependent functions and μ-independent continuous bilinear forms, respectively; and $c^r : X \times X \times L^\infty(\Omega) \to \mathbb{R}$ and $g^r(\cdot;\mu) \in L^\infty(\Omega) \cap C^0(\Omega)$, $1 \leqslant r \leqslant R$, are trilinear forms and prescribed functions, respectively.

We shall make the following assumptions. First, we assume that a is continuous,

$$a(w,v;\mu) \leqslant \Gamma(\mu)\|w\|_X\|v\|_X \leqslant \gamma_0\|w\|_X\|v\|_X, \quad \forall \mu \in \mathcal{D} \tag{18}$$

coercive,

$$0 < \alpha_0 \leqslant \ \alpha(\mu) = \inf_{w \in X} \frac{a(w,w;\mu)}{\|w\|_X^2}, \quad \forall \mu \in \mathcal{D}, \tag{19}$$

and symmetric, $a(w,v;\mu) = a(v,w;\mu), \forall w, v \in X, \forall \mu \in \mathcal{D}$. (We (plausibly) suppose that α_0, Γ_0 may be chosen independent of $\mathcal{N}$.) Second, we assume that the trilinear forms c^r, $1 \leqslant r \leqslant R$, are bounded

$$c^r(w,v,z) \leqslant \gamma_0^r\|w\|_X\|v\|_X\|z\|_{L^\infty(\Omega)}, \quad \forall w, v \in X, \quad \forall z \in L^\infty(\Omega). \tag{20}$$

Third, we assume that our linear forms $f(\cdot)$ and $\ell(\cdot)$ are bounded.

$$f(v) \leqslant \gamma_0^f\|v\|_X, \quad \forall v \in X, \tag{21}$$

$$\ell(v) \leqslant \gamma_0^\ell\|v\|_X, \quad \forall v \in X. \tag{22}$$

It is then standard, under the above assumptions, to prove existence and uniqueness of the exact solution and the truth approximation. Finally, we assume that

$$\ell(v) = f(v), \quad \forall v \in X. \tag{23}$$

Hence, our output functional is "compliant"; more general functionals and nonsymmetric a require adjoint techniques to improve the output convergence [12,24–26].

Before developing the RB approximation and associated *a posteriori* error estimation for this problem, we briefly review the empirical interpolation method [1,2] necessary for the treatment of nonaffine parameter operators of the form (17).

3. Coefficient-function approximation

3.1. Interpolation procedure

We consider the problem of approximating a given μ-dependent function $g(x;\mu) \in L^\infty(\Omega) \cap C^0(\Omega), \ \forall \mu \in \mathcal{D}$, by a coefficient-function expansion $g_M(x;\mu)$. Toward this end, we assume that we are given $M_{\max}$ basis functions, ϕ_m, $1 \leqslant m \leqslant M_{\max}$, and define nested approximation spaces, $W_M^g = \text{span}\{\phi_1, \ldots, \phi_M\}$, $1 \leqslant M \leqslant M_{\max}$. We further assume that we are given associated nested sets of interpolation points $T_M = \{z_1 \in \Omega, \ldots, z_M \in \Omega\}$, $1 \leqslant M \leqslant M_{\max}$.

Next, we define our coefficient-function approximation as

$$g_M(x;\mu) = \sum_{m=1}^{M} \underline{\beta}_{Mm}(\mu)\phi_m(x) \tag{24}$$

where the coefficient vector $\underline{\beta}_M(\mu) = (\underline{\beta}_{M1}(\mu) \ldots \underline{\beta}_{MM}(\mu)) \in \mathbb{R}^M$ is found such that

$$\sum_{m=1}^{M} \phi_m(z_i)\underline{\beta}_{Mm}(\mu) = g(z_i;\mu), \quad i = 1, \ldots, M. \tag{25}$$

We define the associated error as

$$\varepsilon_M(\mu) \equiv \|g(\cdot;\mu) - g_M(\cdot;\mu)\|_{L^\infty(\Omega)}. \tag{26}$$

In words, we find $g_M(\cdot;\mu)$ by interpolating $g(\cdot;\mu)$ at the interpolation points $\{z_m\}_{m=1}^M$.

Often we evaluate the quality of our approximation relative to the "best approximation"

$$g_M^*(\cdot;\mu) = \arg\min_{w\in W_M^g} \|g(\cdot;\mu) - w\|_{L^\infty(\Omega)}. \tag{27}$$

The associated error is defined as

$$\varepsilon_M^*(\mu) \equiv \|g(\cdot;\mu) - g_M^*(\cdot;\mu)\|_{L^\infty(\Omega)}. \tag{28}$$

Note that the best approximation $g_M^*(x;\mu)$ requires the full knowledge of $g(x;\mu)$.

Of course, the approximation quality depends critically both on $\{\phi_m\}_{m=1}^{M_{\max}}$ and $\{z_m\}_{m=1}^{M_{\max}}$. In this paper we use the POD method [21–23] to compute $\{\phi_m\}_{m=1}^{M_{\max}}$ from a suitably fine set of snapshots

$$\mathcal{S}_K^g \equiv \{\xi_k^g(x) = g(x;\mu_k^g), \quad \mu_k^g \in S_K^g, 1 \leqslant k \leqslant K\},$$

where $S_K^g = \{\mu_1^g, \ldots, \mu_K^g\}$ is a large parameter sample set. The POD is detailed in Appendix A for reference. We note that the POD will be expensive if the number of snapshots K is very large. It is thus important to select a small snapshot set with good approximation properties. Often (especially for high-dimensional parameter domains) we combine the POD with the greedy sampling procedure [16,20,19] in our basis construction process. See Section 6 for a detailed discussion.

Once we have the basis set $\{\phi_m\}_{m=1}^{M_{\max}}$, we can determine the point set $\{z_m\}_{m=1}^{M_{\max}}$ by using the empirical interpolation method as follows.

3.2. Empirical interpolation procedure

To begin, we choose the first interpolation point as $z_1 = \arg\max_{x\in\Omega}|\phi_1(x)|$ and compute $\psi_1(x) = \phi_1(x)/\phi_1(z_1)$ and $\underline{B}_1 = 1$. For $M = 2, \ldots, M_{\max}$, we first solve the linear system for $\underline{\sigma}_{M-1,j}$, $1 \leqslant j \leqslant M$, from

$$\sum_{j=1}^{M-1} \psi_j(z_i)\underline{\sigma}_{M-1,j} = \phi_M(z_i), \quad i = 1, \ldots, M-1, \tag{29}$$

and set

$$r_M(x) = \phi_M(x) - \sum_{j=1}^{M-1} \underline{\sigma}_{M-1,j}\psi_j(x); \tag{30}$$

we then define

$$z_M = \arg\max_{x\in\Omega}|r_M(x)|, \tag{31}$$

and compute $\psi_M(x) = r_M(x)/r_M(z_M)$ and $\underline{B}_{M\ ij} = \psi_j(z_i)$, $1 \leqslant i,j \leqslant M$.

It is shown in [1,2] that the functions $\{\psi_1, \ldots, \psi_M\}$ form a basis for W_M^g and that $g_M(x;\mu)$ defined earlier in (24) can be also computed in terms of the ψ_m as

$$g_M(x;\mu) = \sum_{m=1}^{M} \underline{\varphi}_{Mm}(\mu)\psi_m(x), \tag{32}$$

where the coefficient vector $\underline{\varphi}_M(\mu) \in \mathbb{R}^M$ is determined from

$$\sum_{j=1}^{M} \underline{B}_{Mij}\underline{\varphi}_{Mj}(\mu) = g(z_i;\mu), \quad 1 \leqslant i \leqslant M. \tag{33}$$

We shall use interpolation formula (32) and (33) from now on. We note that $\underline{\varphi}_M(\mu)$ requires $O(M^2)$ operations once the inverse matrix $\underline{B}_M^{-1}$ is pre-computed.

Theoretical and numerical aspects of the empirical interpolation have been analyzed in great detail in [1,2]. We summarize here the main results: (i) the process is stable – $\underline{B}_M$ is a well-conditioned lower triangular matrix with dominant unity diagonal; and (ii) the Lebesgue constant is bounded above by $2^M - 1$.[1]

3.3. A posteriori estimators

Given an approximation $g_M(x;\mu)$, we define $\mathcal{E}_M(x;\mu) \equiv \hat{\varepsilon}_M(\mu)\psi_{M+1}(x)$, where $\hat{\varepsilon}_M(\mu) \equiv |g(z_{M+1};\mu) - g_M(z_{M+1};\mu)|$. In general, $\varepsilon_M(\mu) \geqslant \hat{\varepsilon}_M(\mu)$, since $\varepsilon_M(\mu) = \|g(\cdot;\mu) - g_M(\cdot;\mu)\|_{L^\infty(\Omega)} \geqslant |g(x;\mu) - g_M(x;\mu)|$ for all $x \in \Omega$, and thus also for $x = z_{M+1}$. However, we can prove

Proposition 1. *If* $g(\cdot;\mu) \in W^g_{M+1}$, *then* (*i*) $g(x;\mu) - g_M(x;\mu) = \pm\mathcal{E}_M(x;\mu)$, *and* (*ii*) $\|g(\cdot;\mu) - g_M(\cdot;\mu)\|_{L^\infty(\Omega)} = \hat{\varepsilon}_M(\mu)$.

The proof of this proposition was given in [1,2].

Of course, in general $g(\cdot;\mu) \notin W^g_{M+1}$, and hence our estimator $\hat{\varepsilon}_M(\mu)$ is unfortunately a lower bound. However, if $\varepsilon_M(\mu) \to 0$ very fast, we expect that the effectivity,

$$\eta_M(\mu) \equiv \frac{\hat{\varepsilon}_M(\mu)}{\varepsilon_M(\mu)}, \tag{34}$$

shall be close to unity; furthermore, the estimator is very inexpensive – *one additional evaluation* of $g(\cdot;\mu)$ at a single point in Ω.

In the subsequent sections, we shall incorporate our coefficient-function approximation $g_M(x;\mu)$ and associate error estimator $\hat{\varepsilon}_M$ to develop the RB approximation and *a posteriori* error estimation for the field variable $u(\mu)$ and output $s(\mu)$.

4. Reduced-basis approximation

4.1. Affine decomposition

We assume that we are given $N_{\max}$ global basis functions $\{\zeta_n\}_{n=1}^{N_{\max}}$ and associated hierarchical RB spaces $W^u_N = \text{span}\{\zeta_1,\ldots,\zeta_N\}, 1 \leqslant N \leqslant N_{\max}$. In practice, these basis functions are constructed by the basis construction process described in Section 6. We first apply a standard Galerkin projection for the weak form (16) to obtain an approximation $u_N(\mu) \in W^u_N$ from

$$\sum_{q=1}^{Q} \Theta^q_b(\mu) b^q(u_N(\mu), v) + \sum_{r=1}^{R} c^r(u_N(\mu), v, g^r(x;\mu)) = f(v), \quad \forall v \in W^u_N. \tag{35}$$

As mentioned in the Introduction, because of the nonaffine parameter operators $c^r(\cdot,\cdot,g^r(x;\mu))$, $1 \leqslant r \leqslant R$, the online complexity of this standard Galerkin reduced-basis model depends on $\mathcal{N}_t$ – the dimension of the finite element truth approximation space X.

To recover (online) $\mathcal{N}_t$-independent cost, we simply replace $g^r(x;\mu)$, $1 \leqslant r \leqslant R$, with our coefficient-function approximations

$$g^r_{M^r}(x;\mu) = \sum_{m=1}^{M^r} \underline{\varphi}^r_{M^r m}(\mu)\psi^r_m(x), \quad 1 \leqslant r \leqslant R, \tag{36}$$

where

$$\sum_{j=1}^{M^r} \underline{B}^r_{M^r ij}\underline{\varphi}^r_{M^r j}(\mu) = g^r(z^r_i;\mu), \quad 1 \leqslant i \leqslant M^r, \ \ 1 \leqslant r \leqslant R. \tag{37}$$

[1] The bound is very pessimistic and of little practical value. In applications, the actual asymptotic behavior of the Lebesgue constant is much lower than the upper bound $2^M - 1$, typically $O(M)$; however, the bound does provide a theoretical basis for some stability.

Here $\{z_m^r\}_{m=1}^{M^r}$, $\{\psi_m^r\}_{m=1}^{M^r}$, and $\underline{B}^r_{M^r ij} = \psi_j^r(z_i^r), 1 \leqslant r \leqslant R$, are constructed by following the procedures described in Section 3. Let us denote $M = \sum_{r=1}^R M^r$. Our RB approximation is then: given $\mu \in \mathcal{D}$, we evaluate

$$s_{N,M}(\mu) = f(u_{N,M}(\mu)), \tag{38}$$

where $u_{N,M}(\mu) \in W_N^u$ satisfies

$$\sum_{q=1}^{Q} \Theta^q(\mu) b^q(u_{N,M}(\mu), v) + \sum_{r=1}^{R} c^r(u_{N,M}(\mu), v, g^r_{M^r}(x;\mu)) = f(v), \quad \forall v \in W_N^u. \tag{39}$$

We shall develop the offline–online computational decomposition for this RB formulation in Section 4.3.

4.2. A priori theory

We consider the convergence rate of $u_{N,M}(\mu) \to u(\mu)$ and $s_{N,M}(\mu) \to s(\mu)$. In fact, it is a simple matter to demonstrate the optimality of $u_{N,M}(\mu)$ in

Proposition 2. *For* $\varepsilon^r_{M^r}(\mu) \equiv \|g^r(\cdot;\mu) - g^r_{M^r}(\cdot;\mu)\|_{L^\infty(\Omega)}, 1 \leqslant r \leqslant R$, *satisfying* $2\sum_{r=1}^R \varepsilon^r_{M^r}(\mu)\gamma_0^r \leqslant \alpha_0$, *we have*

$$\begin{aligned}\|u(\mu) - u_{N,M}(\mu)\|_X^2 \leqslant \frac{\gamma_0}{\alpha_0} \inf_{w_N \in W_N^u} \|u(\mu) - w_N\|_X^2 + 4\frac{\gamma_0^f}{\alpha_0^2}\left(\sum_{r=1}^R \varepsilon^r_{M^r}(\mu)\gamma_0^r\right) \\ \times \left(\frac{\gamma_0}{\alpha_0} \inf_{w_N \in W_N^u} \|w_N - u(\mu)\|_X + \frac{2\gamma_0^f}{\alpha_0^2}\sum_{r=1}^R \varepsilon^r_{M^r}(\mu)\gamma_0^r\right)\end{aligned} \tag{40}$$

for all $\mu \in \mathcal{D}$.

The proof of this proposition and the following ones are given in Appendix B. We can further show that

Proposition 3. *Assuming the same hypothesis in Proposition 2, we have*

$$|s(\mu) - s_{N,M}(\mu)| \leqslant \gamma_0 \|u(\mu) - u_{N,M}(\mu)\|_X^2 + \left(\frac{2\gamma_0^f}{\alpha_0}\right)^2 \sum_{r=1}^R \varepsilon^r_{M^r}(\mu)\gamma_0^r \tag{41}$$

for all $\mu \in \mathcal{D}$. *Here* $\|u(\mu) - u_{N,M}(\mu)\|_X$ *is bounded by (40) of Proposition 2.*

Propositions 2 and 3 indicate that M should be chosen such that $\varepsilon_M(\mu)$ is square of the error in the best approximation, $\inf_{w_N \in W_N^u} \|u(\mu) - w_N\|_X^2$, as otherwise the second term on the right-hand side of (41) may limit the output convergence. In that case, we expect that the output error $|s(\mu) - s_{N,M}(\mu)|$ will converge as the square of the error norm $\|u(\mu) - u_{N,M}(\mu)\|_X$. As regards the error in the best approximation, we note that W_N^u comprises solutions on the parametrically induced manifold $\mathcal{M}^u \equiv \{u(\mu) | \forall \mu \in \mathcal{D}\} \subset X$. The critical observations are that $\mathcal{M}^u$ is very *low-dimensional* and that $\mathcal{M}^u$ is *smooth* under general hypotheses on stability and continuity. We thus expect that the best approximation will converge to $u(\mu)$ very rapidly, and hence that N may be chosen small. (This is proven for a particularly simple case in [11].)

4.3. Offline–online procedure

We now insert $u_{N,M}(\mu) = \sum_{j=1}^N \underline{u}_{N,Mj}(\mu)\zeta_j$ and (36) into (39) and choose $v = \zeta_i$, $1 \leqslant i \leqslant N$, to obtain

$$\left(\sum_{q=1}^{Q} \Theta^q(\mu)\underline{B}_N^q + \sum_{r=1}^{R}\sum_{m=1}^{M^r} \underline{\varphi}^r_{M^r m}(\mu)\underline{C}_N^{rm}\right)\underline{u}_{N,M}(\mu) = \underline{F}_N, \tag{42}$$

where $\underline{\varphi}^r_{M^r}(\mu) \in \mathbb{R}^{M^r}, 1 \leqslant r \leqslant R$, are determined from (37). We then evaluate

$$s_{N,M}(\mu) = \underline{F}_N^T \underline{u}_{N,M}(\mu). \tag{43}$$

In the above, $\underline{B}_N^q \in \mathbb{R}^{N\times N}$, $\underline{C}_N^{rm} \in \mathbb{R}^{N\times N}$, and $\underline{F}_N^q, \in \mathbb{R}^N$ are given by

$$\begin{aligned}
&\underline{B}_{Nij}^q = b^q(\zeta_j, \zeta_i), \quad 1 \leqslant i,j \leqslant N, \quad 1 \leqslant q \leqslant Q,\\
&\underline{C}_{Nij}^{rm} = c^r(\zeta_j, \zeta_i, \psi_m^r), \quad 1 \leqslant i,j \leqslant N, \quad 1 \leqslant r \leqslant R, \quad 1 \leqslant m \leqslant M^r,\\
&\underline{F}_{Ni} = f(\zeta_i), \quad 1 \leqslant i \leqslant N.
\end{aligned} \tag{44}$$

We proceed to develop the offline–online procedure [12,26,20] for the rapid evaluation of our RB output $s_{N,M}(\mu)$.

In the offline stage, we compute and store the parameter-independent quantities in (44), which require $N_{\max}$ finite element solutions at the selected parameter points and $O(N_{\max} + QN_{\max}^2 + MN_{\max}^2)$ $\mathcal{N}_t$-inner products; recall that $M = \sum_{r=1}^R M^r$. The offline computation is thus expensive, but it is performed only *one time*. (Note here that the offline cost does not include the construction of $\{\psi_m^r\}_{m=1}^{M_{\max}^r}$ and $\{z_m^r\}_{m=1}^{M_{\max}^r}, 1 \leqslant r \leqslant R$.) However, in the online stage – for each new parameter value μ – we compute the vectors $\underline{\varphi}_{M^r}^r(\mu), 1 \leqslant r \leqslant R$, at cost $O(\sum_{r=1}^R (M^r)^2)$, perform the sum in the parentheses and the right-hand side of (42) at cost $\mathcal{O}(QN^2 + MN^2)$, invert the linear system at cost $\mathcal{O}(N^3)$, and evaluate the output $s_N(\mu)$ at cost $\mathcal{O}(N)$. The operation count for the online stage is thus only $\mathcal{O}(\sum_{r=1}^R (M^r)^2 + QN^2 + MN^2 + N^3)$.

Hence, as required in the many-query or real-time contexts, the online complexity is independent of $\mathcal{N}_t$, the dimension of the underlying finite element approximation space. Since $Q, R, N, M^r \ll \mathcal{N}_t$, we expect significant computational savings in the online stage relative to the finite element approximation (16) and relative to the standard Galerkin RB approximation built upon (35).

5. A posteriori error estimation

5.1. Error bounds

We assume that we are given a positive lower bound for the coercivity parameter, $\hat{\alpha}(\mu)$, such that $\alpha(\mu) \geqslant \hat{\alpha}(\mu) > 0, \forall \mu \in \mathcal{D}$. Various recipes for the construction of $\hat{\alpha}(\mu)$ can be found in [12,13]. We introduce the residual for our RB approximation $u_{N,M}(\mu)$ as

$$r(v;\mu) = f(v) - \sum_{q=1}^{Q} \Theta^q(\mu) b^q(u_{N,M}(\mu), v) - \sum_{r=1}^{R} c^r(u_{N,M}(\mu), v, g_{M^r}^r(\cdot;\mu)), \quad \forall v \in X. \tag{45}$$

We can show that

Proposition 4. *Suppose that $g^r(x;\mu) \in W_{M^r+1}^{g^r}, 1 \leqslant r \leqslant R$, then the error $e(\mu) \equiv u(\mu) - u_{N,M}(\mu)$ satisfies*

$$\|e(\mu)\|_X \leqslant \Delta_{N,M}^u(\mu), \quad \forall \mu \in \mathcal{D}, \tag{46}$$

where the error bound $\Delta_{N,M}^u(\mu)$ is defined as

$$\Delta_{N,M}^u(\mu) = \frac{1}{\hat{\alpha}(\mu)} \left(\|r(\cdot;\mu)\|_{X'} + \sup_{v\in X} \frac{\sum_{r=1}^R \hat{\varepsilon}_{M^r}^r(\mu) c^r(u_{N,M}(\mu), v, \psi_{M^r+1}^r)}{\|v\|_X} \right). \tag{47}$$

Here $\hat{\varepsilon}_{M^r}^r(\mu) = |g^r(z_{M^r+1}^r;\mu) - g_{M^r}^r(z_{M^r+1}^r;\mu)|$ is the estimator for the error $\varepsilon_{M^r}^r(\mu), 1 \leqslant r \leqslant R$.

We further obtain the error bound for the output estimate as

Proposition 5. *Suppose that $g^r(x;\mu) \in W_{M^r+1}^{g^r}, 1 \leqslant r \leqslant R$, then the error in the output of interest is bounded by*

$$|s(\mu) - s_{N,M}(\mu)| \leqslant \Delta_{N,M}^s(\mu), \quad \forall \mu \in \mathcal{D}, \tag{48}$$

where $\Delta_{N,M}^s(\mu)$ is defined as

$$\Delta_{N,M}^s(\mu) = \hat{\alpha}(\mu)(\Delta_{N,M}^u(\mu))^2 + \left| \sum_{r=1}^R \hat{\varepsilon}_{M^r}^r(\mu) c^r(u_{N,M}(\mu), u_{N,M}(\mu), \psi_{M^r+1}^r) \right|, \tag{49}$$

and $\Delta_{N,M}^u(\mu)$ is defined in Proposition 4.

Of course, in general $g^r(x;\mu) \notin W^{g^r}_{M^r+1}$, and hence our output bound $\Delta^s_{N,M}(\mu)$ is not completely rigorous. However, if $\varepsilon^r_{M^r}(\mu) \to 0, 1 \leqslant r \leqslant R$, very fast such that the *non-rigorous* part $\left|\sum_{r=1}^R \hat{\varepsilon}^r_{M^r}(\mu) c^r(u_{N,M}(\mu), u_{N,M}(\mu), \psi^r_{M^r+1})\right|$ is relatively small to the *rigorous* part $\hat{\alpha}(\mu)(\Delta^u_{N,M}(\mu))^2$, we recover the *square effect* as for the affine compliant case [11–13]:

$$\Delta^s_{N,M}(\mu) \approx \hat{\alpha}(\mu)(\Delta^u_{N,M}(\mu))^2. \tag{50}$$

Our output bound $\Delta^s_{N,M}(\mu)$ will thus be fully rigorous in the limit $M^r \to \infty$, $1 \leqslant r \leqslant R$. However, if the output bound is not yet rigorous for the current values M^r, $1 \leqslant r \leqslant R$, its rigor can be always consolidated by further increasing M^r albeit at higher computational cost. In practice, we recommend to choose M^r, $1 \leqslant r \leqslant R$, such that the non-rigorous part does not exceed the rigorous part.

It remains to develop the offline–online decomposition for the efficient calculation of $\Delta^u_{N,M}(\mu)$ and $\Delta^s_{N,M}(\mu)$.

5.2. Offline–online procedure

To begin, we invoke our duality argument (12)–(14) to obtain

$$\|r(\cdot;\mu)\|_{X'} \equiv \sup_{v \in X} \frac{r(v;\mu)}{\|v\|_X} = \|\hat{e}(\mu)\|_X, \tag{51}$$

where $\hat{e}(\mu)$ is the solution of

$$(\hat{e}(\mu), v)_X = r(v;\mu), \quad \forall v \in X. \tag{52}$$

From (45) and (52) it follows that $\hat{e}(\mu)$ satisfies

$$(\hat{e}(\mu), v)_X = f(v) - \sum_{q=1}^{Q}\sum_{n=1}^{N} \Theta^q(\mu)\underline{u}_{N,Mn}(\mu) b^q(\zeta_n, v) - \sum_{r=1}^{R}\sum_{m=1}^{M^r}\sum_{n=1}^{N} \underline{\varphi}^r_{M^r m}(\mu)\underline{u}_{N,Mn}(\mu) c^r(\zeta_n, v, \psi^r_m), \quad \forall v \in X. \tag{53}$$

It is clear from linear superposition that we can express $\hat{e}(\mu)$ as

$$\hat{e}(\mu) = \mathcal{L}_f + \sum_{q=1}^{Q}\sum_{n=1}^{N} \Theta^q(\mu)\underline{u}_{N,Mn}(\mu)\mathcal{L}^{qn}_b + \sum_{r=1}^{R}\sum_{m=1}^{M^r}\sum_{n=1}^{N} \underline{\varphi}^r_{M^r m}(\mu)\underline{u}_{N,Mn}(\mu)\mathcal{L}^{rmn}_c, \tag{54}$$

where

$$\begin{aligned} &(\mathcal{L}_f, v)_X = f(v), \quad \forall v \in X, \\ &(\mathcal{L}^{qn}_b, v)_X = -b^q(\zeta_n, v), \quad \forall v \in X, \\ &(\mathcal{L}^{mn}_c, v)_X = -c^r(\zeta_n, v, \psi^r_m), \quad \forall v \in X, \end{aligned} \tag{55}$$

for $1 \leqslant q \leqslant Q$, $1 \leqslant r \leqslant R$, $1 \leqslant m \leqslant M^r$, $1 \leqslant n \leqslant N$; note that these are simple parameter-independent (scalar or vector) Poisson, or Poisson-like, problems.

From (51) and (54) it follows that

$$\begin{aligned} \|r(\cdot;\mu)\|^2_{X'} = {} & \Lambda_{ff} + \sum_{q=1}^{Q}\sum_{n=1}^{N} \Theta^q(\mu)\underline{u}_{N,Mn}(\mu)\Lambda^{qn}_{fb} + \sum_{r=1}^{R}\sum_{m=1}^{M^r}\sum_{n=1}^{N} \underline{\varphi}^r_{M^r m}(\mu)\underline{u}_{N,Mn}(\mu)\Lambda^{rmn}_{fc} \\ & + \sum_{q=1}^{Q}\sum_{n=1}^{N}\sum_{q'=1}^{Q}\sum_{n'=1}^{N} \Theta^q(\mu)\underline{u}_{N,Mn}(\mu)\Theta^{q'}(\mu)\underline{u}_{N,Mn'}(\mu)\Lambda^{qnq'n'}_{bb} \\ & + \sum_{q=1}^{Q}\sum_{n=1}^{N}\sum_{r=1}^{R}\sum_{m=1}^{M^r}\sum_{n'=1}^{N} \Theta^q(\mu)\underline{u}_{N,Mn}(\mu)\underline{\varphi}^r_{M^r m}(\mu)\underline{u}_{N,Mn'}(\mu)\Lambda^{qnrmn'}_{bc} \\ & + \sum_{r=1}^{R}\sum_{m=1}^{M^r}\sum_{n=1}^{N}\sum_{r'=1}^{R}\sum_{m'=1}^{M^r}\sum_{n'=1}^{N} \underline{\varphi}^r_{M^r m}(\mu)\underline{u}_{N,Mn}(\mu)\underline{\varphi}^{r'}_{M^{r'} m'}(\mu)\underline{u}_{N,Mn'}(\mu)\Lambda^{rmnr'm'n'}_{cc} \end{aligned} \tag{56}$$

where the parameter-independent quantities Λ are defined as

$$\begin{aligned}
\Lambda_{ff} &= (\mathcal{L}_f, \mathcal{L}_f)_X, \\
\Lambda_{fb}^{qn} &= 2(\mathcal{L}_f, \mathcal{L}_b^{qn})_X, \\
\Lambda_{fc}^{rmn} &= 2(\mathcal{L}_f, \mathcal{L}_c^{rmn})_X \\
\Lambda_{bb}^{qnq'n'} &= (\mathcal{L}_b^{qn}, \mathcal{L}_b^{q'n'})_X, \quad \Lambda_{bc}^{qnrmn'} = 2(\mathcal{L}_b^{qn}, \mathcal{L}_c^{rmn'})_X, \\
\Lambda_{cc}^{rmnr'm'n'} &= (\mathcal{L}_c^{rmn}, \mathcal{L}_c^{r'm'n'})_X,
\end{aligned} \tag{57}$$

for $1 \leqslant q,q' \leqslant Q$, $1 \leqslant r,r' \leqslant R$, $1 \leqslant m,m' \leqslant M^r$, $1 \leqslant n,n' \leqslant N$. Similarly, we obtain

$$\sup_{v \in X} \frac{\sum_{r=1}^{R} \hat{\varepsilon}_{M^r}^r(\mu) c^r(u_{N,M}(\mu), v, \psi_{M^r+1}^r)}{\|v\|_X} = \|\hat{e}_c(\mu)\|_X, \tag{58}$$

where

$$\|\hat{e}_c(\mu)\|_X^2 = \sum_{r=1}^{R} \sum_{n=1}^{N} \sum_{r'=1}^{R} \sum_{n'=1}^{N} \hat{\varepsilon}_{M^r}^r(\mu) \underline{u}_{N,Mn}(\mu) \hat{\varepsilon}_{M^{r'}}^{r'}(\mu) \underline{u}_{N,Mn'}(\mu) \Lambda_{cc}^{rnr'n'}; \tag{59}$$

here, for $1 \leqslant r,r' \leqslant R$, $1 \leqslant n,n' \leqslant N$,

$$(\mathcal{L}_c^{rn}, v)_X = c^r(\zeta_n, v, \psi_{M^r+1}^r), \quad \forall v \in X, \tag{60}$$

$$\Lambda_{cc}^{rnr'n'} = (\mathcal{L}_c^{rn}, \mathcal{L}_c^{r'n'})_X, \tag{61}$$

which are parameter-independent quantities. Furthermore, the nonrigorous part of the output bound can be expressed as

$$\sum_{r=1}^{R} \hat{\varepsilon}_{M^r}^r(\mu) c^r(u_{N,M}(\mu), u_{N,M}(\mu), \psi_{M^r+1}^r) = \sum_{r=1}^{R} \sum_{n=1}^{N} \sum_{n'=1}^{N} \hat{\varepsilon}_{M^r}^r(\mu) \underline{u}_{N,Mn}(\mu) \underline{u}_{N,Mn'}(\mu) \Lambda_c^{rnn'}, \tag{62}$$

where, for $1 \leqslant r \leqslant R$, $1 \leqslant n,n' \leqslant N$,

$$\Lambda_c^{rnn'} = c^r(\zeta_n, \zeta_{n'}, \psi_{M^r+1}^r) \tag{63}$$

are parameter-independent quantities.

The offline–online decomposition is now clear. In the offline stage – performed only once – we first compute the vectors $\mathcal{L}$ from (55) and (60), and then form the scalar quantities Λ from (57), (61) and (63); this requires $(1 + QN + MN)$ Poisson solutions and $(1 + QN + MN + Q^2N^2 + QMN^2 + M^2N^2)$ $\mathcal{N}_t$-inner products. In the online stage – given a new parameter value μ and associated RB vector $\underline{u}_{N,M}(\mu)$ – the operation count to perform the sums (56), (59), and (62) is $O(Q^2N^2 + M^2N^2)$; the online storage is $O(Q^2N^2 + M^2N^2)$. Hence, the online calculation of $\Delta_{N,M}^u(\mu)$ and $\Delta_{N,M}^s(\mu)$ is independent of $\mathcal{N}_t$.

6. Basis adaptivity

The *a posteriori* error bounds certainly play a crucial role in providing reliable estimation for quantities of interest in applications. Our *a posteriori* error bounds also allow us to pursue an "optimal" construction of the hierarchical RB spaces $W_N^u = \text{span}\{\zeta_1, \ldots, \zeta_N\}$, $1 \leqslant N \leqslant N_{\max}$, at greatly low average cost. The crucial point is that $\Delta_{N,M}^s(\mu)$ is an accurate yet "online-inexpensive" surrogate for the true (very-expensive-to-calculate) error $|s(\mu) - s_{N,M}(\mu)|$. We can thus conduct an extensive search over the parameter space to find the optimal set of snapshots upon which our basis set shall be constructed by using the POD procedure. In essence, our basis construction process combines the greedy sampling procedure [16,20,19] and the POD procedure [21–23].

First, we pursue the adaptive sampling procedure to select an optimal sampling set $S_{N_{\max}}^u = \{\mu_1^u, \ldots, \mu_{N_{\max}}^u\}$. We assume that we are given an initial parameter set $S_N^u = \{\mu_1^u, \ldots, \mu_N^u\}$, and hence associated Lagrange approximation space $W_N^{u,\text{Lag}} = \text{span}\{\zeta_n^{\text{Lag}} = u(\mu_n^u), 1 \leqslant n \leqslant N\}$. We also assume that the basis sets $\{\psi_m^r\}_{m=1}^{M_{\max}^r}$ and interpolation point sets $\{z_m^r\}_{m=1}^{M_{\max}^r}$, $1 \leqslant r \leqslant R$, are available. (Often we shall initialize $N = 1$ and $M^r = M_{\max}^r - 1$, and choose μ_1^u randomly.) We set our RB space W_N^u to be $W_N^{u,\text{Lag}}$ and solve

$$\mu^u_{N+1} = \arg\max_{\mu\in\mathcal{D}} \Delta^s_{N,M}(\mu); \tag{64}$$

we next append μ^u_{N+1} to S^u_N to form S^u_{N+1}, and hence associated Lagrange space $W^{u,\mathrm{Lag}}_{N+1} = W^{u,\ \mathrm{Lag}}_N + \mathrm{span}\{u(\mu^u_{N+1})\}$; we then increment $N = N+1$ and repeat the process until $N = N_{\max}$ such that $\epsilon^*_{N_{\max}} = \epsilon_{\mathrm{tol,min}}$, where $\epsilon^*_N = \Delta^s_{N,M}(\mu^u_N), 1 \leqslant N \leqslant N_{\max}$. Here $\epsilon_{\mathrm{tol,min}}$ is the smallest error tolerance anticipated *a priori* offline.

Second, we apply the POD (in Appendix A) on the snapshot set $\mathcal{S}^u_{N_{\max}} = \{u(\mu^u_1), \ldots, u(\mu^u_{N_{\max}})\}$ to obtain a POD basis set $\{\zeta^{\mathrm{POD}}_n\}^{N_{\max}}_{n=1}$. We define associated nested POD approximation spaces as $W^{u,\ \mathrm{POD}}_N = \mathrm{span}\{\zeta^{\mathrm{POD}}_1, \ldots, \zeta^{\mathrm{POD}}_N\}, 1 \leqslant N \leqslant N_{\max}$. We must then also compute parameter-independent quantities for the POD basis set $\{\zeta_n^{\ \mathrm{POD}}\}^{N_{\max}}_{n=1}$, following the offline–online procedures described in Sections 4.3 and 5.2. We note that the POD spaces are not in general Lagrange, since one POD basis function is a linear combination of $N_{\max}$ Lagrange basis functions. We have of course $W^{u,\mathrm{POD}}_{N_{\max}} = W^{u,\mathrm{Lag}}_{N_{\max}}$, but in general $W^{u,\mathrm{POD}}_N \neq W^{u,\mathrm{Lag}}_N$ for $N < N_{\max}$.

After this point, we can consider $W^u_N = W^{u,\mathrm{POD}}_N$ for the online evaluation of the output $s_{N,M}(\mu)$ and error bound $\Delta^s_{N,M}(\mu)$ for any given new μ. The justification for choosing POD spaces over Lagrange spaces lies in the optimality property of $W^{u,\mathrm{POD}}_N$ for all $N \leqslant N_{\max}$. Furthermore, as mentioned in Appendix A, the POD spaces are also orthonormal and hierarchical. These properties are very important for good convergence behavior of the RB approximation (related to optimal), well-conditioned RB system (related to orthonormal), and efficient offline/online decomposition (related to hierarchical).

In this paper, the MATLAB® genetic algorithm toolbox is used to solve the maximization problem (64). We start the genetic search process with a small (random or deterministic) sample set over the parameter domain and let it evolve until either the objective value is no longer improved in a few iterations or the maximum number of iterations is exceeded. We note that the problem (64) is typically non-convex with many local optima. This is because when a new parameter point μ^u_{N+1} is selected, the error bound $\Delta^s_{N+1,M}(\mu)$ becomes effectively zero at the point μ^u_{N+1}, thereby creating new local optima in the parameter space. This effect in turn introduces many more local optima as N increases. Hence, we do not claim that our basis construction process is truly optimal, as the global maximizer of (64) may not be reached by the genetic algorithm. However, genetic algorithms as global search heuristics prove very well-suited to global optimization problems such as the problem (64). Gradient or Hessian-based optimization methods with multi-start strategies can be also used to solve (64), but such methods require the derivatives of $\Delta^s_{N,M}(\mu)$.

Instead of solving (64) directly, the greedy approach [16,20,19] finds $\mu^u_{N+1} = \max_{\mu\in\Xi_{\mathrm{train}}} \Delta^s_{N,M}(\mu)$; here $\Xi_{\mathrm{train}} = \{\mu^{\mathrm{train}}_1, \ldots, \mu^{\mathrm{train}}_{n_{\mathrm{train}}}\}$ is a suitably *fine* training set of size n_{train} over the parameter domain $\mathcal{D}$. The greedy approach relies on the finesse of the training set and the inexpensive RB error surrogate $\Delta^s_{N,M}(\mu)$ to find a good sample set. However, as n_{train} may scale *exponentially* with the dimension of the parameter space, the greedy approach appears quite prohibitive for high-dimensional parameter spaces even with the RB error surrogate $\Delta^s_{N,M}(\mu)$.

Finally, we would like to point out that without inexpensive error surrogates the usual POD reduced order model techniques [27–38] typically construct $N_{\max}$ POD basis functions from the training snapshot set $\mathcal{S}^u{}_{\mathrm{train}} = \{u(\mu^{\mathrm{train}}_1), \ldots, u(\mu^{\mathrm{train}}_{n_{\mathrm{train}}})\}$. The associated offline work requires n_{train} finite element solutions, $n_{\mathrm{train}}(n_{\mathrm{train}}+1)/2$ $\mathcal{N}^t$-inner products, and a singular value decomposition of a $n_{\mathrm{train}} \times n_{\mathrm{train}}$ *full* symmetric positive-definite matrix for $N_{\max}$ leading eigenvalues and eigenvectors. Such basis construction approach can thus be extremely expensive (much more than the greedy approach and our proposed approach) when n_{train} is relatively large compared to $N_{\max}$. Other approaches (such as goal-oriented, model-constrained optimization framework) [39] suffer from similar drawbacks.

7. Numerical application

7.1. Problem description

We turn to a particular problem related to steady heat conduction. We consider the design of a heat shield, one segment of which is shown in Fig. 1. The original domain Ω_o, a typical point of which is (x^1_o, x^2_o), is given

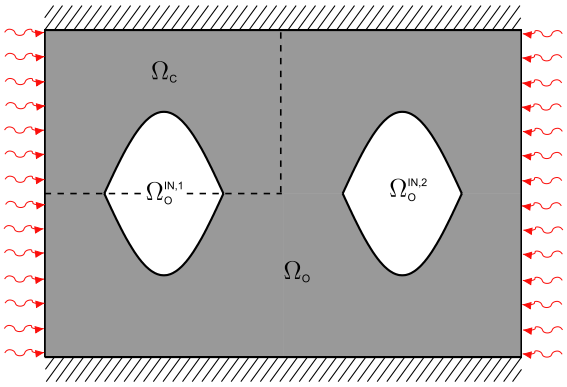

Fig. 1. One segment of the heat shield. The "cut" domain Ω_c is one quarter of the heat shield.

by $\Omega_o \equiv]-3+L, 1+L[\times]-1, 1[\backslash\{\overline{\Omega}_o^{in,1} \cup \overline{\Omega}_o^{in,2}\}$; here $\Omega_o^{in,1}$ and $\Omega_o^{in,2}$ are open sinusoidal domains parametrized by the length parameters H and L. The left and right boundaries, Γ_o^{out}, are exposed to a hot temperature normalized to unity; the top and bottom boundaries are insulated. The heat conduction through the internal boundaries Γ_o^{in} (i.e., the surfaces of the two ellipse cooling channels $\Omega_o^{in,1} \cup \Omega_o^{in,2}$) to the surrounding flowing air is characterized by a zero sink temperature and non-dimensional heat transfer coefficient (Biot number) Bi. Our input parameter vector is hence $\mu \equiv (\mu^1, \mu^2, \mu^3) \equiv (L, H, Bi) \in \mathcal{D} \equiv [0.25, 0.75]^2 \times [0.1, 5] \subset \mathbb{R}^{P=3}$. The physical model is simple conduction: the non-dimensional temperature field in the shield, u_o^e, satisfies

$$\int_{\Omega_o} \nabla u_o^e \cdot \nabla v + Bi \int_{\Gamma_o^{in}} u_o^e v = \int_{\Gamma_o^{out}} v, \quad \forall v \in X_o^e \equiv H^1(\Omega_o). \tag{65}$$

Our output is the average temperature of the left and right boundaries.

We next exploit the symmetry to recast the problem into one quarter of the original domain, Ω_c, as shown in Fig. 2(a). The non-dimensional temperature field u_c^e on the domain Ω_c thus satisfies

$$\int_{\Omega_c} \nabla u_c^e \cdot \nabla v + Bi \int_{\Gamma_c^{in}} u_c^e v = \int_{\Gamma_c^{out}} v, \quad \forall v \in X_c^e \equiv H^1(\Omega_c). \tag{66}$$

The output of interest is given by $s_c^e(\mu) = \int_{\Gamma_c^{out}} u_c^e(\mu)$. Note Γ_c^{out} is the interval $0 \leqslant x^2 \leqslant 1$ at $x^1 = -1 + L$ and Γ_c^{in} is the sinusoidal curve $x_c^2 = H \sin(\pi x_c^1/2L)$ for $0 \leqslant x_c^1 \leqslant 2L$.

We now introduce a fixed reference domain $\Omega \equiv]-0.5, 1.5[\times]0, 1[$ as shown in Fig. 2b. We decompose $\Omega_c(\mu)$ and Ω as

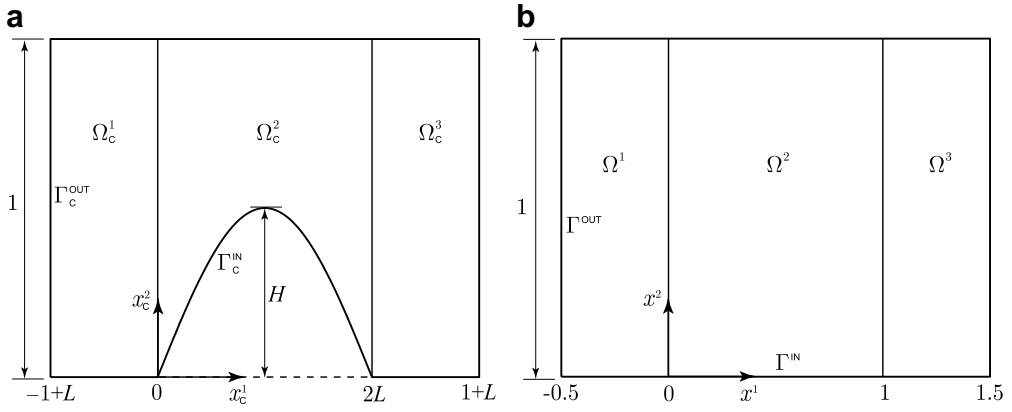

Fig. 2. Domain decomposition for: (a) the cut domain Ω_c and (b) the reference domain Ω.

$$\overline{\Omega}_c(\mu) = \overline{\Omega}^1_c(\mu) \cup \overline{\Omega}^2_c(\mu) \cup \overline{\Omega}^3{}_c(\mu), \quad \overline{\Omega} = \overline{\Omega}^1 \cup \overline{\Omega}^2 \cup \overline{\Omega}^3, \tag{67}$$

where $\Omega^1{}_c(\mu) \equiv]-1+\mu^1, 0[\times]0,1[, \Omega^3_c(\mu) \equiv]2\mu^1, 1+\mu^1[\times]0,1[, \Omega^2_c(\mu) \equiv \Omega_c(\mu) \setminus \{\overline{\Omega}^1_c(\mu) \cup \overline{\Omega}^3_c(\mu)\}, \Omega^1 \equiv]-0.5, 0[\times]0,1[, \Omega^2 \equiv]0,1[\times]0,1[, \Omega^3 \equiv]1, 1.5[\times]0,1[$. We then define a geometric transformation $\mathcal{F}$ from $x = (x^1, x^2) \in \Omega$ to $x_c = (x^1_c, x^2_c) \in \Omega_c$: the mapping from Ω^1 to Ω^1_c is *affine* as

$$x^1_c = \frac{(1-\mu^1)}{0.5}(x^1 + 0.5) + \mu^1 - 1, \quad x^2_c = x^2; \tag{68}$$

the mapping from Ω^2 to Ω^2_c is *nonaffine* as

$$x^1_c = 2\mu^1 x^1, \quad x^2_c = x^2 + \mu^2(1-x^2)\sin(\pi x^1); \tag{69}$$

and the mapping from Ω^3 to Ω^3_c is *affine* as

$$x^1_c = \frac{(1-\mu^1)}{0.5}(x^1 - 1.0) + 2\mu^1, \quad x^2_c = x^2. \tag{70}$$

We proceed to formulate the problem on the reference domain.

Our exact solution on the original cut domain $\Omega_c(\mu), u^e_c(x_c;\mu)$, can be expressed in terms of the solution on the mapped domain, $u^e(x;\mu)$, as $u^e_c(x_c;\mu) = u^e(\mathcal{F}(x_c);\mu)$. The solution on the mapped domain, $u^e(x;\mu) \in X^e \equiv H^1(\Omega)$, satisfies a weak formulation of the form (15)–(17) in which the linear forms, bilinear forms, trilinear forms, and nonaffine functions are given by

$$f(v) = \ell(v) = \int_{\Gamma^{\text{out}}} v, \tag{71}$$

$$\begin{aligned}
\Theta^1(\mu) &= \frac{1}{2-2\mu^1}, \quad b^1(w,v) = \int_{\Omega^1\cup\Omega^3} \frac{\partial w}{\partial x^1}\frac{\partial v}{\partial x^1}, \\
\Theta^2(\mu) &= 2-2\mu^1, \quad b^2(w,v) = \int_{\Omega^1\cup\Omega^3} \frac{\partial w}{\partial x^2}\frac{\partial v}{\partial x^2}, \\
\Theta^3(\mu) &= \frac{1}{2\mu^1}, \quad b^3(w,v) = \int_{\Omega^2} \frac{\partial w}{\partial x^1}\frac{\partial v}{\partial x^1}, \\
\Theta^4(\mu) &= -\frac{\mu^2}{2\mu^1}, \quad b^4(w,v) = \int_{\Omega^2} \sin(\pi x)\frac{\partial w}{\partial x^1}\frac{\partial v}{\partial x^1} + \pi(1-y)\cos(\pi x)\left(\frac{\partial w}{\partial x^1}\frac{\partial v}{\partial x^2} + \frac{\partial w}{\partial x^2}\frac{\partial v}{\partial x^1}\right),
\end{aligned} \tag{72}$$

for Θ^q and b^q, $1 \leqslant q \leqslant Q = 4$; and

$$\begin{aligned}
c^1(w,v,g^1(x;\mu)) &= \int_{\Omega^2} g^1(x;\mu)\frac{\partial w}{\partial x^2}\frac{\partial v}{\partial x^2}, \\
g^1(x;\mu) &= \frac{\pi^2(\mu^2)^2(1-x^2)^2\cos^2(\pi x^1) + 4(\mu^1)^2}{2\mu^1(1-\mu^2\sin(\pi x^1))}, \\
c^2(w,v,g^2(x;\mu)) &= \int_{\Gamma^{\text{in}}} g^2(x;\mu) wv, \\
g^2(x;\mu) &= \mu^3\sqrt{4(\mu^1)^2 + \pi^2(\mu^2)^2\cos^2(\pi x^1)}
\end{aligned} \tag{73}$$

for $c^r(w,v,g^r(x;\mu))$ and $g^r(x;\mu)$, $1 \leqslant r \leqslant R = 2$. Note that the functions $g^1(x;\mu)$ and $g^2(x;\mu)$ are defined on Ω^2 and Γ_{in}, respectively; and that they are *nonaffine* only in the parameters μ^1 and μ^2.

For our truth approximations $u(\mu)$ and $s(\mu)$, we consider a linear finite element approximation subspace $X \in H^1(\Omega)$ of dimension $\mathcal{N}_t = 4753$. We define the associated inner product as

$$(w,v)_X \equiv \sum_{q=1}^{Q} \Theta(\overline{\mu}_1) b^q(w,v) + c^1(w,v,g^1(x;\overline{\mu}_1)) + c^2(w,v,g(x;\overline{\mu}_2)), \tag{74}$$

where $\overline{\mu}_1 = (0.75, 0.75, 0.01)$ and $\overline{\mu}_2 = (0.25, 0.25, 0.01)$. We can then choose $\hat{\alpha}(\mu) = 1$ for which it is readily shown that $\hat{\alpha}(\mu) \leqslant \alpha(\mu), \forall \mu \in \mathcal{D}$.

We show in Fig. 3 the temperature variation over the heat shield for different parameter values. We note that for smaller values of μ^3 the temperature is, overall, much higher than for larger values of μ^3; and that the temperature field varies significantly with the shape of the heat shield. In the next section, we present numerical results obtained for the above problem.

7.2. Numerical results

We first present results for the coefficient-function approximation of $g^1(x;\mu)$ and $g^2(x;\mu)$. We choose for S_K^g a deterministic grid of 15×15 parameter points over $\mathcal{D}^g \equiv [0.25, 0.75]^2 \subset \mathbb{R}^{P=2}$ and then pursue the POD and the empirical interpolation procedure described in Section 2 to construct $\{z_m^1\}_{m=1}^{M_{\max}^1=15}$, $\{\psi_m^1\}_{m=1}^{M_{\max}^1=15}$ for $g^1(x;\mu)$ and $\{z_m^2\}_{m=1}^{M_{\max}^2=9}$, $\{\psi_m^2\}_{m=1}^{M_{\max}^2=9}$ for $g^2(x;\mu)$. We show in Fig. 4 the locations of $z_m^1, 1 \leqslant m \leqslant M_{\max}^1$, on the subdomain Ω^2. We observe that all the interpolation points line up along the bottom and top boundaries of Ω^2. This is because $g^1(x;\mu)$ varies most significantly along these boundaries.

For convergence study, we introduce a parameter test sample Ξ_{Test}^g over $\mathcal{D}^g$ of size $n_{\text{Test}}^g = 961$, and define

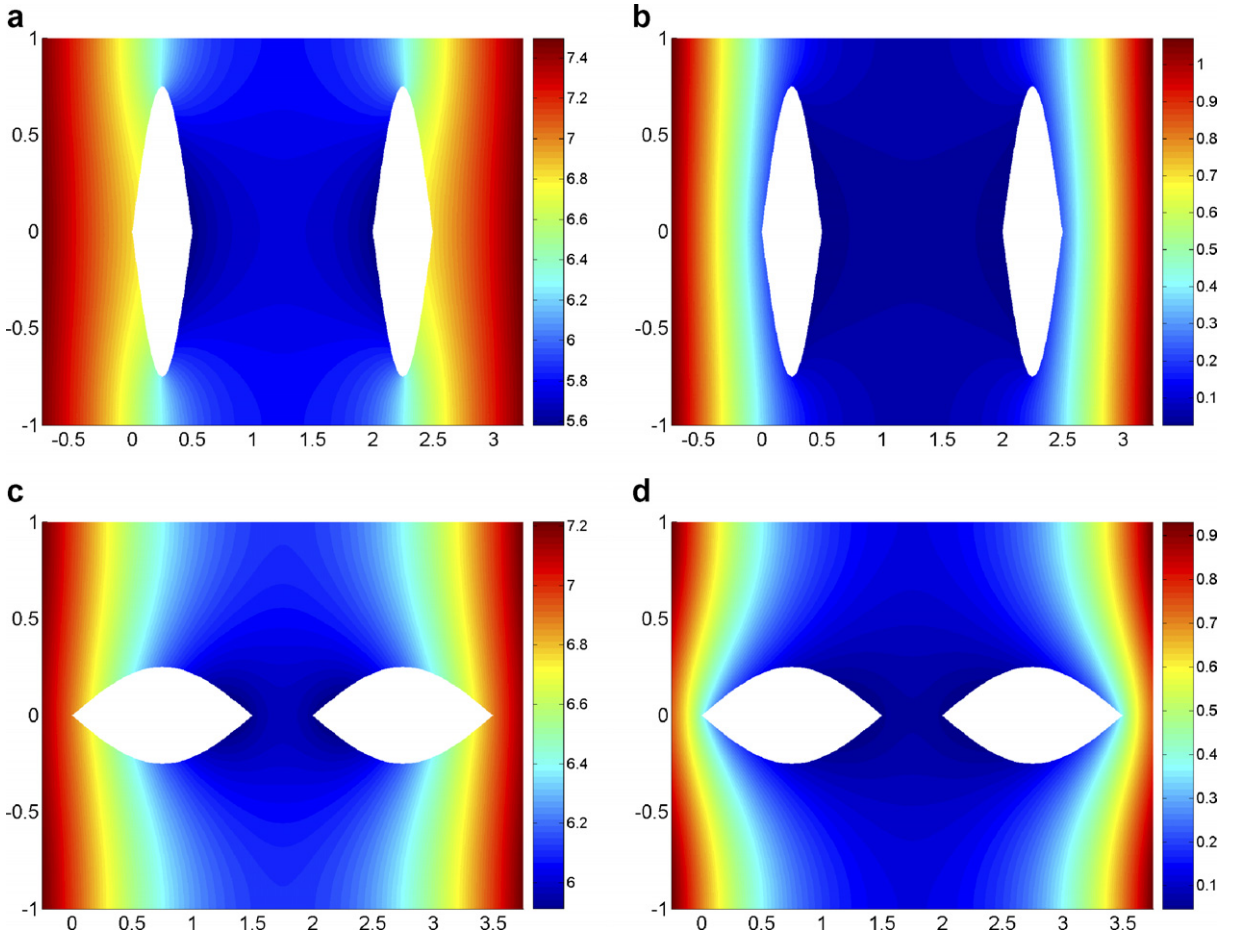

Fig. 3. Temperature in the heat shield for: (a) $\mu = (0.25, 0.75, 0.1)$; (b) $\mu = (0.25, 0.75, 5)$; (c) $\mu = (0.75, 0.25, 0.1)$; and (d) $\mu = (0.75, 0.25, 5)$.

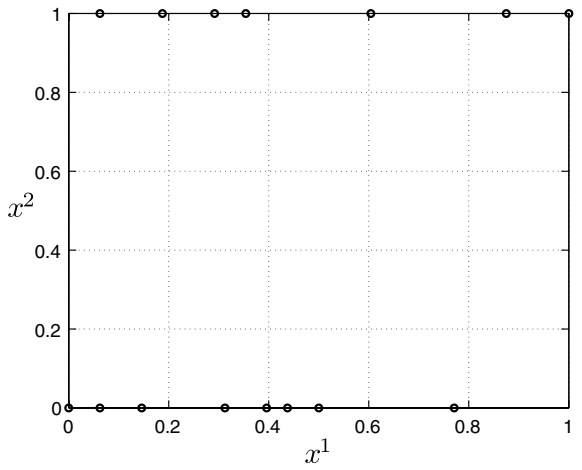

Fig. 4. Interpolation points z^1_m, $1 \leqslant m \leqslant M^1_{\max} = 15$, for the function $g^1(x;\mu)$.

$$
\begin{aligned}
\varepsilon^r_{M^r,\max,\mathrm{rel}} &= \max_{\mu\in\Xi^g_{\mathrm{Test}}} \frac{\varepsilon^r_{M^r}(\mu)}{\|g^r(x;\mu)\|_{L^\infty(\Omega^2)}},\\
\varepsilon^{r*}_{M^r,\max,\mathrm{rel}} &= \max_{\mu\in\Xi^g_{\mathrm{Test}}} \frac{\varepsilon^{r*}_{M^r}(\mu)}{\|g^r(x;\mu)\|_{L^\infty(\Omega^2)}},\\
\Upsilon^r_{M^r,\mathrm{ave}} &= \frac{1}{n^g_{\mathrm{Test}}} \sum_{\mu\in\Xi^g_{\mathrm{Test}}} \frac{\varepsilon^r_{M^r}(\mu)}{\varepsilon^{r*}_{M^r}(\mu)},\\
\eta^r_{M^r,\mathrm{ave}} &= \frac{1}{n^g_{\mathrm{Test}}} \sum_{\mu\in\Xi^g_{\mathrm{Test}}} \eta^r_{M^r}(\mu),
\end{aligned}
\tag{75}
$$

for $1 \leqslant r \leqslant R$; here $\eta^r_{M^r}(\mu)$ is the effectivity defined in (34). We present $\varepsilon^r_{M^r,\max,\ \mathrm{rel}}$, $\varepsilon^{r*}_{M^r,\max,\mathrm{rel}}$, $\Upsilon^r_{M^r,\mathrm{ave}}$, and $\eta^r_{M^r,\mathrm{ave}}$ as a function of M^r in Table 1 for $r = 1$ and in Table 2 for $r = 2$. We observe in both cases that $\varepsilon^r_{M^r,\max,\mathrm{rel}}$ and $\varepsilon^{r*}_{M^r,\max,\mathrm{rel}}$ converge rapidly with M^r; that $\Upsilon^r_{M^r,\mathrm{ave}}$ are quite close to unity–and hence $\varepsilon^r_{M^r}(\mu)$ will be only slightly larger than $\varepsilon^{r*}_{M^r}(\mu)$; and that the error estimator effectivities are quite close to unity.

We next present results for our basis generation. We choose our first sample point $\mu^u_1 = (0.25, 0.25, 0.1)$ and set $\epsilon_{\mathrm{tol,min}} = 1\mathrm{E}{-}06$. In the course of solving the problem (64) repeatedly, we initialize the genetic algorithm with a small regular grid of size $3\times3\times3$ over the parameter domain $\mathcal{D}$ and set the maximum number of iterations to 20. We plot the resulting sampling set $S^u_{N_{\max}} = \{\mu^u_n, 1 \leqslant n \leqslant N_{\max}\}$ in Fig. 5 – we need $N_{\max} = 34$ basis functions to obtain the desired accuracy. Note that for this problem our basis construction algorithm selects many sample points on the planes $\mu^3 = 0.1$ and $\mu^3 = 5$. Fig. 6 illustrates that $\Delta^s_{N,M}(\mu)$ is indeed non-convex with many local maxima. Furthermore, we show in Fig. 7 the maximum value of the objective function as a function of N for the proposed sampling method and greedy sampling method. Here the greedy sampling is performed on a fine regular grid of size $n_{\mathrm{train}} = 15\times15\times15$ over the parameter domain. We see that while the two methods yield very similar results, the number of output evaluations is 540 for the proposed method and 3375 for the greedy method. We should anticipate that the number of output evaluations will increase for higher-dimensional parameter spaces. Nevertheless, in such cases, the proposed sampling method appears much more efficient since it can provide good snapshots with a significantly smaller number of output evaluations.

We now present numerical results for the RB approximation and *a posteriori* error estimation. For this purpose, we introduce a parameter test sample Ξ^u_{Test} over $\mathcal{D}$ of size $n^u_{\mathrm{Test}} = 512$, and define

$$
\begin{aligned}
\epsilon^u_{N,M,\max} &= \max_{\mu\in\Xi^u_{\mathrm{Test}}} \|u(\mu) - u_{N,M}(\mu)\|_X,\\
\epsilon^s_{N,M,\max} &= \max_{\mu\in\Xi^u_{\mathrm{Test}}} |s(\mu) - s_{N,M}(\mu)|.
\end{aligned}
\tag{76}
$$

Table 1
Numerical results for empirical interpolation of $g^1(x;\mu)$: $\varepsilon^{1*}_{M^1,\max,\mathrm{rel}}$, $\varepsilon^{1}_{M^1,\max,\mathrm{rel}}$, $\Upsilon^1_{M^1,\mathrm{ave}}$, and $\eta^1_{M^1,\mathrm{ave}}$ as a function of M^1

M^1	$\varepsilon^{1*}_{M^1,\max,\mathrm{rel}}$	$\varepsilon^{1}_{M^1,\max,\mathrm{rel}}$	$\Upsilon^1_{M^1,\mathrm{ave}}$	$\eta^1_{M^1,\mathrm{ave}}$
2	2.45E−01	3.03E−01	1.09	0.81
4	2.30E−02	4.42E−02	1.58	0.72
6	2.22E−03	3.17E−03	1.24	0.67
8	1.91E−04	2.88E−04	1.61	0.79
10	1.37E−05	4.47E−05	3.69	0.90
12	8.36E−07	1.36E−06	1.69	0.79
14	2.54E−07	4.12E−07	1.12	0.98

Table 2
Numerical results for empirical interpolation of $g^2(x;\mu)$: $\varepsilon^{2*}_{M^2,\max,\mathrm{rel}}$, $\varepsilon^{2}_{M^2,\max,\mathrm{rel}}$, $\Upsilon^2_{M^2,\mathrm{ave}}$, and $\eta^2_{M^2,\mathrm{ave}}$ as a function of M^2

M^2	$\varepsilon^{2*}_{M^2,\max,\mathrm{rel}}$	$\varepsilon^{2}_{M^2,\max,\mathrm{rel}}$	$\Upsilon^2_{M^2,\mathrm{ave}}$	$\eta^2_{M^2,\mathrm{ave}}$
1	2.77E−01	3.62E−01	1.28	0.97
2	2.29E−02	2.97E−02	1.45	0.94
3	2.79E−03	3.38E−03	1.31	0.91
4	3.59E−04	6.12E−04	2.16	0.97
5	4.64E−05	7.82E−05	1.63	0.96
6	5.76E−06	8.44E−06	1.78	0.93
7	7.09E−07	1.15E−06	1.79	0.94
8	9.30E−08	2.34E−07	2.33	0.90

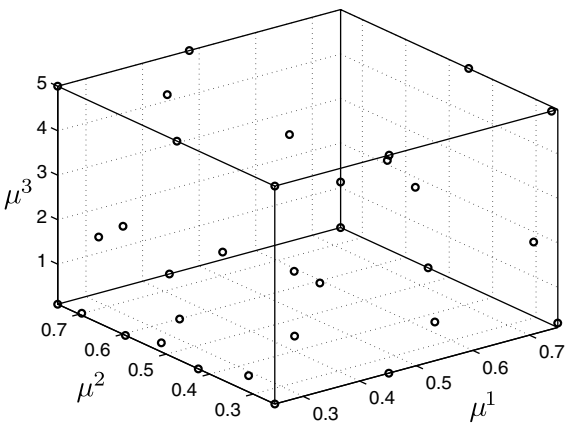

Fig. 5. Distribution of the sampling set $S^u_{N_{\max}} = \{\mu^u_n, 1 \leqslant n \leqslant N_{\max} = 34\}$ over the parameter space.

We present in Fig. 8(a) $\epsilon^s_{N,M,\max}$ as a function of N for different values of (M^1, M^2). We observe very rapid convergence of $s_{N,M}(\mu)$ to $s(\mu)$. Clearly, the quality of the output approximation depends on N and (M^1, M^2) in a strongly coupled manner: for a fixed value of the pair (M^1, M^2) the error decreases with N for small N and then levels off for N large enough; when the error does not improve with increasing N, increasing (M^1, M^2) effectively reduces the error. This trend of convergence basically suggests that optimal combinations of N and (M^1, M^2) are at the "knees" of the error curves. It is important to note that our coefficient-function approximations to the nonaffine functions are very accurate such that both M^1 and M^2 can be chosen optimally smaller than N. We further illustrate in Fig. 8(b) that $\epsilon^s_{N,M,\max}$ is effectively the square of $\epsilon^u_{N,M,\max}$ for (sufficiently large) $M^1 = 14$ and $M^2 = 8$ for which the errors $\varepsilon^1_{M^1,\max,\mathrm{rel}}$ and $\varepsilon^2_{M^2,\max,\mathrm{rel}}$ are below $\epsilon_{\mathrm{tol,min}} = 1.0\mathrm{E}{-}06$ as indicated in Tables 1 and 2. These results are consistent with our *a priori* convergence analysis of Section 4.2.

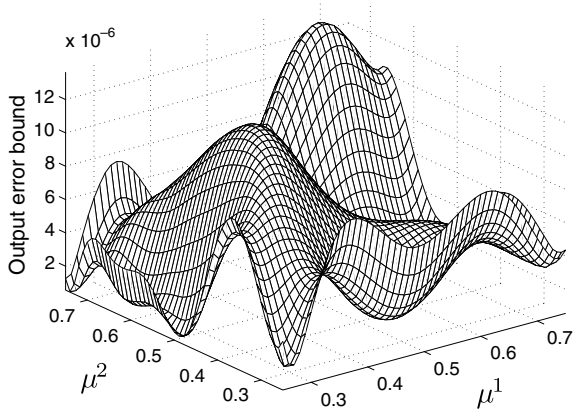

Fig. 6. $\Delta^s_{N,M}(\mu)$ as a function of μ^1 and μ^2 for a fixed value of $\mu^3 = 0.1$ for $N = 20$, $M^1 = 14$, and $M^2 = 8$.

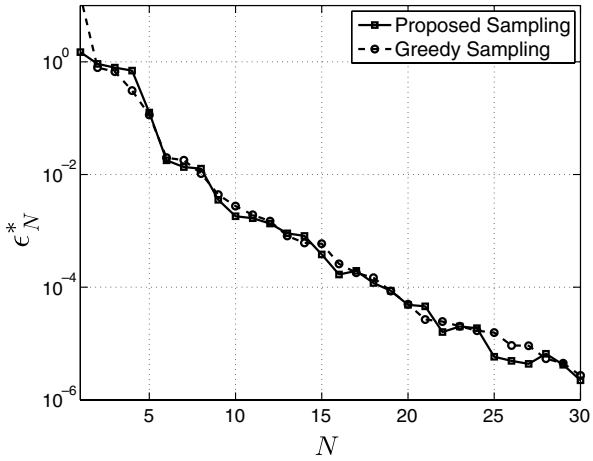

Fig. 7. The maximum value of the objective function, $\epsilon^*_N = \Delta_{N,M}(\mu^*_N)$, as a function of N for the proposed sampling method and greedy sampling method.

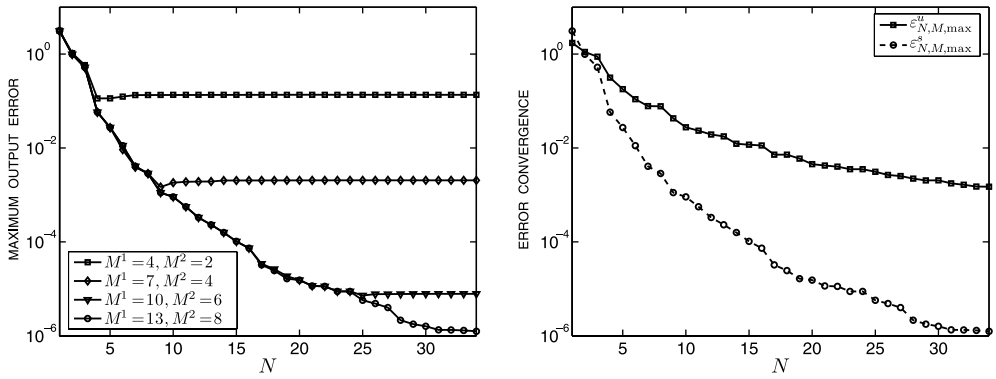

Fig. 8. Convergence of the RB errors: (a) $\epsilon^s_{N,M,\max}$ as a function of N for different values of M^1 and M^2; and (b) $\epsilon^s_{N,M,\max}$ and $\epsilon^u_{N,M,\max}$ as a function of N for $M^1 = 14$ and $M^2 = 8$.

Furthermore, in order to evaluate the performance of the error bounds, we define

$$\begin{aligned}
\eta^s_{N,M,\text{ave}} &= \frac{1}{n^u_{\text{Test}}} \sum_{\mu\in\Xi^u_{\text{Test}}} \frac{\Delta^s_{N,M}(\mu)}{|s(\mu) - s_{N,M}(\mu)|},\\
\eta^s_{N,M,\text{min}} &= \min_{\mu\in\Xi^u_{\text{Test}}} \frac{\Delta^s_{N,M}(\mu)}{|s(\mu) - s_{N,M}(\mu)|},\\
\Delta^u_{N,M,\text{max,rel}} &= \max_{\mu\in\Xi^u_{\text{Test}}} \frac{\Delta^u_{N,M}(\mu)}{\|u(\mu)\|_X},\\
\Delta^s_{N,M,\text{max,rel}} &= \max_{\mu\in\Xi^u_{\text{Test}}} \frac{\Delta^s_{N,M}(\mu)}{|s(\mu)|}.
\end{aligned} \tag{77}$$

We present $\eta^s_{N,M,\text{ave}}$ in Fig. 9a and $\eta^s_{N,M,\text{min}}$ in Fig. 9b as a function of N for different values of (M^1, M^2). The average output effectivity $\eta^s_{N,M,\text{ave}}$ is above unity and less than 6 for all N. However, as we may expect, the minimum output effectivity $\eta^s_{N,M,\text{min}}$ (above 0.2) is less than but not far off unity. Hence, our output error bound $\Delta^s_{N,M}(\mu)$ is very sharp, but not fully rigorous. We further tabulate in Table 3 $\Delta^u_{N,M,\text{max,rel}}$ and $\Delta^s_{N,M,\text{max, rel}}$ for different values of (N, M^1, M^2). We observe very rapid convergence of the error bounds. Also, $\Delta^s_{N,M,\text{max,rel}}$ converges roughly as the square of $\Delta^u_{N,M,\text{max,rel}}$.

Finally, in Table 4, we present the online computational times to calculate $s_{N,M}(\mu)$ and $\Delta^s_{N,M}(\mu)$. The values are normalized with respect to the computational time for the direct calculation of the truth approximation output

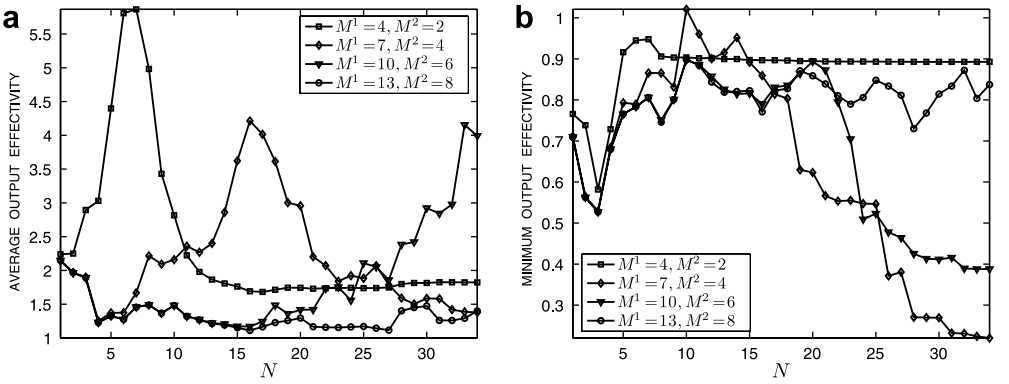

Fig. 9. Output effectivity: (a) $\eta^s_{N,M,\text{ave}}$; and (b) $\eta^s_{N,M,\text{min}}$ as a function of N for different values of (M^1, M^2).

Table 3
Convergence rate of the error bounds: $\Delta^u_{N,M,\text{max,rel}}$ and $\Delta^s_{N,M,\text{max, rel}}$ for different values of (N, M^1, M^2)

N	M^1	M^2	$\Delta^u_{N,M,\text{max,rel}}$	$\Delta^s_{N,M,\text{max,rel}}$
5	3	2	2.33E−01	5.06E−02
10	5	3	3.65E−02	1.08E−03
15	7	4	1.57E−02	2.71E−04
20	9	5	4.74E−03	2.22E−05
25	11	6	2.44E−03	5.13E−06
30	13	7	1.06E−03	9.79E−07

Table 4
Online computational times (normalized with respect to the time to solve for $s(\mu)$)

N	M^1	M^2	$s_{N,M}(\mu)$	$\Delta^s_{N,M}(\mu)$	$s(\mu)$
5	3	2	1.40E−04	4.66E−05	1
10	5	3	1.63E−04	1.16E−04	1
15	7	4	1.86E−04	3.96E−04	1
20	9	5	2.33E−04	1.05E−03	1
25	11	6	2.79E−04	2.00E−03	1
30	13	7	3.03E−04	3.98E−03	1

$s(\mu)$. We observe significant computational savings: for a relative accuracy of approximately 0.1 percent in the output approximation corresponding to $(N, M^1, M^2) = (10, 5, 3)$ in Table 3, the reduction in time is more than a factor of 3500 owing to the dramatic dimension reduction provided by the Galerkin projection on the reduced space W_N^u and coefficient-function approximations for the nonaffine terms. Of course, this comparison is only meaningful if we are in the real-time or many-query contexts (for example, in-the-field design and optimization) – in which the extensive offline computations can be amortized over many output predictions.

8. Conclusions

We have presented *a posteriori* error estimation and basis adaptivity for reduced-basis approximation of nonaffine-parametrized linear elliptic PDEs. Numerical results indicate that the approach provides rapid convergence and sharp error bounds for the output of interest relevant to many engineering problems that require repeated output simulations as in the design and optimization context. Nevertheless, several questions arise and remain to be addressed for our approach and, in a larger context, for reduced order modeling of parametrized PDEs. As a first question: can we make our output error bound $\Delta_{N,M}^s(\mu)$ more rigorous? Although quite sharp and very efficient, the error estimators are rigorous upper bounds only in certain restricted situations, i.e., only if the assumption $g(\cdot;\mu) \in W_{M+1}^g$ is satisfied. It turns out that we can readily improve the rigor of our output error bound at only modest additional cost: if we assume that $g(\cdot;\mu) \in W_{M+k}^g$, then $\hat{\varepsilon}_M(\mu) \equiv 2^{k-1}\max_{i\in\{1,\ldots,k\}}|g(z_{M+i};\mu) - g_M(z_{M+i};\mu)|$ is an upper bound for $\varepsilon_M(\mu)$ [2]. However, the most satisfactory answer to this question lies in completely rigorous upper bounds for $\varepsilon_M(\mu)$ without any further assumption on $g(\cdot;\mu)$. Therefore, future work should address this issue.

As the second question: How many parameters P can we consider – for P how large are our techniques still viable? It is undeniably the case that ultimately we should anticipate exponential scaling of N as P increases, with a concomitant unacceptable increase certainly in offline but also perhaps in online computational effort. Fortunately, for smaller P, the growth in N is rather modest, as (good) sampling procedures will automatically identify the more interesting regions of parameter space. For example, the work by Sen [40] has demonstrated the application of reduced-basis methods to "many-parameter" problems involving a few tens of parameters. In any event, treatment of hundreds (or even many tens) of truly independent parameters by the global methods described here is clearly not practicable; in such cases, more local approaches must be pursued.

We close by noting that the offline aspects of the approaches described are both complicated and computationally expensive. The former can be at least partially addressed by appropriate software and architectures [41,42]; however, the latter will in any event remain. It follows that these techniques will really only be viable in situations in which there is truly an imperative for real-time certified response: a real premium on (i) greatly reduced marginal cost (or asymptotic average cost), and (ii) rigorous characterization of certainty. There are many classes of engineering problems and contexts for which the model reduction methods are appropriate; and certainly there are many classes of engineering problems and contexts for which more classical methods remain distinctly preferred.

Acknowledgments

The author thanks Professor Yvon Maday of University of Paris VI, Professor A.T. Patera and Professor J. Paraire of MIT for many invaluable contributions to this work. The author would also like to thank Dr. T. Bui-Thanh, Dr. G.S.H. Pau, Dr. S. Sen, Dr. G. Rozza all from MIT, and Mr. D.B.P. Huynh from National University of Singapore for fruitful discussions. He acknowledges the financial support provided by Professor A.T. Patera and Professor J. Peraire.

Appendix A. Proper orthogonal decomposition

We describe the POD to generate an optimal (in the mean square error sense) basis set $\{\zeta_n^{\mathrm{POD}}\}_{n=1}^N$ from any given (parameter-correlated) set of $K(\geqslant N)$ snapshots $\{\xi_k\}_{k=1}^K$. Our below derivation is a classical result of [21–23].

Let $V_N = \text{span}\{v_1, \ldots, v_N\}$ be an "arbitrary" space of dimension N, the POD space, $W_N^{\text{POD}} = \text{span}\{\zeta_1^{\text{POD}}, \ldots, \zeta_N^{\text{POD}}\}$, is defined as

$$W_N^{\text{POD}} = \arg\inf_{V_N} \left(\frac{1}{K} \sum_{k=1}^{K} \inf_{\underline{\alpha}^k \in \mathbb{R}^N} \left\| \xi_k - \sum_{n=1}^{N} \underline{\alpha}_n^k v_n \right\|_X^2 \right). \tag{A.1}$$

Without loss of generality, we assume that the space V_N is orthonormal – $(v_n, v_m)_X = \delta_{nm}$, $1 \leqslant n,m \leqslant N$. It follows that $\underline{\alpha}_n^k = (\xi_k, v_n)_X, 1 \leqslant n \leqslant N, 1 \leqslant k \leqslant K$, and hence we have

$$W_N^{\text{POD}} = \arg\inf_{V_N} \left(\frac{1}{K} \sum_{k=1}^{K} \left\| \xi_k - \sum_{n=1}^{N} (\xi_k, v_n)_X v_n \right\|_X^2 \right), \tag{A.2}$$

subject to the constraints $(v_n, v_{n'})_X = \delta_{nn'}, 1 \leqslant n, n' \leqslant N$. We then expand the objective and invoke the orthornormality of the space V_N to obtain

$$W_N^{\text{POD}} = \arg\sup_{V_N} \sum_{n=1}^{N} \left(\frac{1}{K} \sum_{k=1}^{K} (\xi_k, v_n)_X^2 \right), \tag{A.3}$$

subject to the constraints $(v_n, v_{n'})_X = \delta_{nn'}, 1 \leqslant n, n' \leqslant N$.

By application of the Euler–Lagrange formulation, the problem (A.3) amounts to solve the eigenproblem,

$$\begin{aligned} &\sum_{k=1}^{K} \frac{1}{K} (\xi_k, \zeta^{\text{POD}})_X (\xi_k, v)_X = \lambda (\zeta^{\text{POD}}, v)_X, \quad \forall v \in X, \\ &(\zeta^{\text{POD}}, \zeta^{\text{POD}})_X = 1, \end{aligned} \tag{A.4}$$

for the first N eigenfunctions $\zeta_n^{\text{POD}}, 1 \leqslant n \leqslant N$, corresponding to the first N largest eigenvalues $\lambda_1 \geqslant \lambda_2 \geqslant \ldots \geqslant \lambda_N$. We note however that the eigenproblem (A.3) posed in the finite element approximation space X of dimension $\mathcal{N}^t$ is quite expensive.

In practice, we typically have $K < \mathcal{N}^t$ (anticipated in the limit $\mathcal{N}^t \to \infty$), we apply the method of snapshots [23] to express a typical empirical eigenfunction ζ^{POD} as a linear combination of the snapshots

$$\zeta^{\text{POD}} = \sum_{k=1}^{K} \underline{a}^k \xi_k. \tag{A.5}$$

Inserting this representation into (A.4) and choosing $v = \xi_i$, $1 \leqslant i \leqslant K$, we immediately obtain

$$\underline{C}\underline{a} = \lambda \underline{a}, \tag{A.6}$$

where $\underline{C} \in \mathbb{R}^{K \times K}$ is a symmetric positive-definite matrix with entries $C_{ij} = \frac{1}{K}(\xi_i, \xi_j)_X, 1 \leqslant i, j \leqslant K$. The eigenproblem (A.6) can then be solved for the first N largest eigenvalues, $\lambda_1 \geqslant \lambda_2 \geqslant \ldots \geqslant \lambda_N$, and corresponding eigenvectors $\underline{a}_n$, $1 \leqslant n \leqslant N$. Finally, the POD basis functions are computed as $\zeta_n^{\text{POD}} = \sum_{k=1}^{K} \underline{a}_n^k \xi_k, 1 \leqslant n \leqslant N$.

From the above construction it should be clear that POD spaces are not only optimal and orthonormal, but also hierarchical – $W_1^{\text{POD}} \subset W_2^{\text{POD}} \subset \cdots \subset W_N^{\text{POD}}$. Also, more generally, the POD can work in other Banach spaces such as $L^2(\Omega)$.

Appendix B. Proof of the propositions

B.1. Proof of proposition 2

Proof. For any $w_N = u_{N,M}(\mu) + v_N \in W_N^u$, $v_N \neq 0$, we have

$$\begin{aligned} a(u(\mu) - w_N, u(\mu) - w_N; \mu) &= a(u(\mu) - u_{N,M}(\mu), u(\mu) - u_{N,M}(\mu); \mu) - 2a(u(\mu) - u_{N,M}(\mu), v_N; \mu) \\ &\quad + a(v_N, v_N; \mu) \\ &\geqslant a(u(\mu) - u_{N,M}(\mu), u(\mu) - u_{N,M}(\mu); \mu) - 2a(u(\mu) - u_{N,M}(\mu), v_N; \mu), \end{aligned} \tag{B.1}$$

since a is symmetric and coercive. We next note from (16), (17), (39), and (20) that

$$
\begin{aligned}
a(u(\mu)-u_{N,M}(\mu),v_N;\mu) &= f(v_N)-a(u_{N,M}(\mu),v_N;\mu)\\
&= f(v_N)-\sum_{q=1}^{Q}\Theta^q(\mu)b^q(u_{N,M}(\mu),v_N)-\sum_{r=1}^{R}c^r(u_{N,M}(\mu),v_N,g^r_{M^r}(\cdot;\mu))\\
&\quad-\sum_{r=1}^{R}c^r(u_{N,M}(\mu),v_N,g^r(\cdot;\mu)-g^r_{M^r}(\cdot;\mu))\\
&\leqslant \sum_{r=1}^{R}\varepsilon^r_{M^r}(\mu)\Gamma^r_0\|u_{N,M}(\mu)\|_X\|v_N\|_X. \qquad \text{(B.2)}
\end{aligned}
$$

Similarly, it follows from (19), (17), (39), (21), and (20) that

$$
\begin{aligned}
\alpha_0\|u_{N,M}(\mu)\|^2_X &\leqslant a(u_{N,M}(\mu),u_{N,M}(\mu);\mu)=f(u_{N,M}(\mu))+\sum_{r=1}^{R}c^r(u_{N,M}(\mu),u_{N,M}(\mu),g^r(\cdot;\mu)-g^r_{M^r}(\cdot;\mu))\\
&\leqslant \Gamma^f_0\|u_{N,M}(\mu)\|_X+\sum_{r=1}^{R}\varepsilon^r_{M^r}(\mu)\Gamma^r_0\|u_{N,M}(\mu)\|^2_X,
\end{aligned}
$$

which yields

$$
\|u_{N,M}(\mu)\|_X \leqslant \frac{2\Gamma^f_0}{\alpha_0} \qquad \text{(B.3)}
$$

after invoking our hypothesis on $\varepsilon_M(\mu)$.

Furthermore, it follows from (19), (18), and (B.2) that

$$
\begin{aligned}
\alpha_0\|v_N\|^2_X=\alpha_0\|w_N-u_{N,M}(\mu)\|^2_X &\leqslant a(w_N-u_{N,M}(\mu),w_N-u_{N,M}(\mu);\mu)\\
&= a(w_N-u(\mu),v_N;\mu)+a(u(\mu)-u_{N,M}(\mu),v_N;\mu)\\
&\leqslant \Gamma_0\|w_N-u(\mu)\|_X\|v_N\|_X+\sum_{r=1}^{R}\varepsilon^r_{M^r}(\mu)\Gamma^r_0\|u_{N,M}(\mu)\|_X\|v_N\|_X
\end{aligned}
$$

which, after dividing by $\alpha_0\|v_N\|_X$ and appealing to (B.3), gives

$$
\|v_N\|_X \leqslant \frac{\Gamma_0}{\alpha_0}\|w_N-u(\mu)\|_X+\frac{2\Gamma^f_0}{\alpha^2_0}\sum_{r=1}^{R}\varepsilon^r_{M^r}(\mu)\Gamma^r_0. \qquad \text{(B.4)}
$$

Finally, gathering (19), (18), (B.1), and (B.2), we obtain

$$
\begin{aligned}
\alpha_0\|u(\mu)-u_{N,M}(\mu)\|^2_X &\leqslant a(u(\mu)-u_{N,M}(\mu),u(\mu)-u_{N,M}(\mu);\mu)\\
&\leqslant a(u(\mu)-w_N,u(\mu)-w_N;\mu)+2a(u(\mu)-u_{N,M}(\mu),v_N;\mu)\\
&\leqslant \Gamma_0\|u(\mu)-w_N\|^2_X+2\sum_{r=1}^{R}\varepsilon^r_{M^r}(\mu)\Gamma^r_0\|u_{N,M}(\mu)\|_X\|v_N\|_X \qquad \text{(B.5)}
\end{aligned}
$$

The desired result follows directly from (B.3)–(B.5). □

B.2. Proof of proposition 3

Proof. We just apply the compliance assumption $\ell = f$, (16), symmetry of a, (18), and (B.2) to obtain

$$
\begin{aligned}
s(\mu)-s_{N,M}(\mu) &= f(u(\mu)-u_{N,M}(\mu);\mu)=a(u(\mu),u(\mu)-u_{N,M}(\mu);\mu)\\
&= a(u(\mu)-u_{N,M}(\mu),u(\mu)-u_{N,M}(\mu);\mu)+a(u(\mu)-u_{N,M}(\mu),u_{N,M}(\mu);\mu)\\
&\leqslant \Gamma_0\|u(\mu)-u_{N,M}(\mu)\|^2_X+\sum_{r=1}^{R}\varepsilon^r_{M^r}(\mu)\Gamma^r_0\|u_{N,M}(\mu)\|^2_X. \qquad \text{(B.6)}
\end{aligned}
$$

The desired result then follows from (B.3). □

B.3. Proof of proposition 4

Proof. We first note from (16), (17), and (45) that $e(\mu)$ satisfies

$$a(e(\mu), v; \mu) = r(v; \mu) - \sum_{r=1}^{R} c^r(u_{N,M}(\mu), v, g^r(\cdot;\mu) - g^r_{M^r}(\cdot;\mu)), \quad \forall v \in X. \tag{B.7}$$

The result immediately follows from

$$\begin{aligned}\|e(\mu)\|_X &\leqslant \frac{1}{\alpha(\mu)} \frac{a(e(\mu), e(\mu); \mu)}{\|e(\mu)\|_X} \leqslant \frac{1}{\hat{\alpha}(\mu)} \frac{r(e(\mu);\mu) - \sum_{r=1}^{R} c^r(u_{N,M}(\mu), e(\mu), g^r(\cdot;\mu) - g^r_{M^r}(\cdot;\mu))}{\|e(\mu)\|_X} \\ &\leqslant \frac{1}{\hat{\alpha}(\mu)} \left(\|r(\cdot;\mu)\|_{X'} + \sup_{v \in X} \frac{\sum_{r=1}^{R} \hat{\varepsilon}^r_{M^r}(\mu) c^r(u_{N,M}(\mu), v, \psi^r_{M^r+1})}{\|v\|_X} \right) = \Delta^u_{N,M}(\mu)\end{aligned} \tag{B.8}$$

where we have used a-coercivity in the first step, $\hat{\alpha}(\mu) \leqslant \alpha(\mu)$ and (B.7) in the second step, and our assumption $g^r(\cdot;\mu) \in W^{g^r}_{M^r+1}$ and Proposition 1 in the last step. □

B.4. Proof of proposition 5

Proof. We first note from (B.6) and (B.2) that

$$\begin{aligned}s(\mu) - s_{N,M}(\mu) &= a(e(\mu), e(\mu); \mu) + a(e(\mu), u_{N,M}(\mu); \mu) \\ &= a(e(\mu), e(\mu); \mu) - \sum_{r=1}^{R} c^r(u_{N,M}(\mu), u_{N,M}(\mu), g^r(\cdot;\mu) - g^r_{M^r}(\cdot;\mu)).\end{aligned} \tag{B.9}$$

It thus follows from (B.9), (B.8), our assumption $g^r(\cdot;\mu) \in W^g_{M+1}$ and Proposition 1 that

$$|s(\mu) - s_{N,M}(\mu)| \leqslant \hat{\alpha}(\mu) \Delta^u_{N,M}(\mu) \|e(\mu)\|_X + \left| \sum_{r=1}^{R} \hat{\varepsilon}^r_{M^r}(\mu) c^r(u_{N,M}(\mu), u_{N,M}(\mu), \psi^r_{M^r+1}) \right|. \tag{B.10}$$

The desired result follows from Proposition 4. □

References

[1] M. Barrault, Y. Maday, N.C. Nguyen, A.T. Patera, An empirical interpolation method: application to efficient reduced-basis discretization of partial differential equations, C.R. Acad. Sci. Paris, Série I 339 (2004) 667–672.

[2] M.A. Grepl, Y. Maday, N.C. Nguyen, A.T. Patera, Efficient reduced-basis treatment of nonaffine and nonlinear partial differential equations, M2AN Math. Model. Numer. Anal. 41 (3) (2007) 575–605.

[3] B.O. Almroth, P. Stern, F.A. Brogan, Automatic choice of global shape functions in structural analysis, AIAA J. 16 (1978) 525–528.

[4] J.P. Fink, W.C. Rheinboldt, On the error behavior of the reduced basis technique for nonlinear finite element approximations, Z. Angew. Math. Mech. 63 (1983) 21–28.

[5] M.D. Gunzburger, Finite Element Methods for Viscous Incompressible Flows: A Guide to Theory, Practice, and Algorithms, Academic Press, Boston, 1989.

[6] K. Ito, S.S. Ravindran, A reduced-order method for simulation and control of fluid flows, J. Comput. Phys. 143 (2) (1998) 403–425.

[7] L. Machiels, Y. Maday, I.B. Oliveira, A.T. Patera, D. Rovas, Output bounds for reduced-basis approximations of symmetric positive definite eigenvalue problems, C.R. Acad. Sci. Paris, Série I 331 (2) (2000) 153–158.

[8] A.K. Noor, J.M. Peters, Reduced basis technique for nonlinear analysis of structures, AIAA J. 18 (4) (1980) 455–462.

[9] J.S. Peterson, The reduced basis method for incompressible viscous flow calculations, SIAM J. Sci. Stat. Comput. 10 (4) (1989) 777–786.

[10] T.A. Porsching, Estimation of the error in the reduced basis method solution of nonlinear equations, Math. Comput. 45 (172) (1985) 487–496.

[11] Y. Maday, A.T. Patera, G. Turinici, Global a priori convergence theory for reduced-basis approximation of single-parameter symmetric coercive elliptic partial differential equations, C.R. Acad. Sci. Paris, Série I 335 (3) (2002) 289–294.

[12] C. Prud'homme, D. Rovas, K. Veroy, Y. Maday, A.T. Patera, G. Turinici, Reliable real-time solution of parametrized partial differential equations: reduced-basis output bound methods, J. Fluids Eng. 124 (1) (2002) 70–80.

[13] K. Veroy, D. Rovas, A.T. Patera, *A posteriori* error estimation for reduced-basis approximation of parametrized elliptic coercive partial differential equations: "Convex inverse" bound conditioners, Control Optimis. Calc. Variat. 8 (2002) 1007–1028 (Special Volume: A tribute to J.-L. Lions).
[14] K. Veroy, A.T. Patera, Certified real-time solution of the parametrized steady incompressible Navier–Stokes equations; rigorous reduced-basis *a posteriori* error bounds, Int. J. Numer. Methods Fluids 47 (2004) 773–788.
[15] K. Veroy, C. Prud'homme, A.T. Patera, Reduced-basis approximation of the viscous Burgers equation: rigorous *a posteriori* error bounds, C.R. Acad. Sci. Paris, Série I 337 (9) (2003) 619–624.
[16] K. Veroy, C. Prud'homme, D.V. Rovas, A.T. Patera, *A posteriori* error bounds for reduced-basis approximation of parametrized noncoercive and nonlinear elliptic partial differential equations (AIAA Paper 2003-3847), in: Proceedings of the 16th AIAA Computational Fluid Dynamics Conference, 2003.
[17] M.A. Grepl, N.C. Nguyen, K.A.T. Patera, G.R. Liu, Certified rapid solution of parametrized partial differential equations for real-time applications, in: Proceedings of the 2nd Sandia Workshop of PDE-Constrained Optimization: Towards Real-Time and On-Line PDE-Constrained Optimization, SIAM Computational Science and Engineering Book Series, 2007, pp. 197–212.
[18] E. Cancès, C. LeBris, Y. Maday, N.C. Nguyen, A.T. Patera, G.S.H. Pau, Feasibility and competitiveness of a reduced basis approach for rapid electronic structure calculations in quantum chemistry, in: Proceedings of the Montreal Workshop for High-dimensional Partial Differential Equations in Science and Engineering, CRM proceedings series, vol. 41, American Mathematical Society, 2007, pp. 15–47.
[19] M.A. Grepl, A.T. Patera, Reduced-basis approximation for time-dependent parametrized partial differential equations, M2AN Math. Model. Numer. Anal. 39 (2005) 157–181.
[20] N.C. Nguyen, K. Veroy, A.T. Patera, Certified real-time solution of parametrized partial differential equations, in: S. Yip (Ed.), Handbook of Materials Modeling, Springer, 2005, pp. 1523–1559.
[21] K. Karhunen, Zur spektraltheorie stochastischer prozesse, Annales Academiae Scientiarum Fennicae 37, 1946.
[22] M.M. Loeve, Probability Theory, Van Nostrand, 1955.
[23] L. Sirovich, Turbulence the dynamics of coherent structures part 1: Coherent structures, Quart. Appl. Math. 45 (3) (1987) 561–571.
[24] Y. Maday, A.T. Patera, D.V. Rovas, A blackbox reduced-basis output bound method for noncoercive linear problems, in: D. Cioranescu, J.-L. Lions, (Eds.), Nonlinear Partial Differential Equations and Their Applications, Collége de France Seminar Volume XIV, Elsevier Science B.V., 2002, pp. 533–569.
[25] N.C. Nguyen, Reduced-basis approximations and a posteriori error bounds for nonaffine and nonlinear partial differential equations: application to inverse analysis, Ph.D. Thesis, Singapore-MIT Alliance, National University of Singapore, Singapore, 2005.
[26] S. Sen, K. Veroy, D. Huynh, S. Deparis, N. Nguyen, A. Patera, natural norm a posteriori error estimators for reduced basis approximations, J. Comput. Phys. 217 (2006) 37–62.
[27] K. Kunisch, S. Volkwein, Control of burgers equation by a reduced order approach using proper orthogonal decomposition, J Optimiz. Theory Appl. 102 (1999) 345–371.
[28] W.R. Graham, J. Peraire, K.Y. Tang, Optimal control of vortex shedding using low order models – Part I: Open-loop model development, Int. J. Numer. Methods Eng. 44 (1999) 945–972.
[29] W.R. Graham, J. Peraire, K.Y. Tang, Optimal control of vortex shedding using low order models – Part II: Model based control, Int. J. Numer. Methods Eng. 44 (1999) 973–990.
[30] S.S. Ravindaran, A reduced-order approach for optimal control of fluids using proper orthogonal decomposition, Int. J. Numer. Meth. Fluids 34 (2000) 425–448.
[31] E. Christensen, M. Brøns, J. Sørensen, Evaluation of proper orthogonal decomposition-based decomposition techniques applied to parameter-dependent nonturbulent flows, SIAM J. Sci. Comput. 21 (4) (2000) 1419–1434.
[32] J.A. Atwell, B.B. King, Proper orthogonal decomposition for reduced basis feedback controllers for parabolic equations, Math. Comput. Model. 33 (1–3) (2001) 1–19.
[33] K. Willcox, J. Peraire, Balanced model reduction via the proper orthogonal decomposition, AIAA 40 (11) (2002) 2323.
[34] M. Meyer, H.G. Matthies, Efficient model reduction in non-linear dynamics using the Karhunen–Loève expansion and dual-weighted-residual methods, Comput. Mech. 31 (1–2) (2003) 179–191.
[35] T. Bui-Thanh, M. Damodaran, K. Willcox, Aerodynamic data reconstruction and inverse design using proper orthogonal decomposition, AIAA 42 (8) (2004) 1505–1516.
[36] C.W. Rowley, T. Colonius, R.M. Murray, Model reduction for compressible flows using pod and Galerkin projection, Physica D: Nonlinear Phenom. 189 (1–2) (2004) 115–129.
[37] M. Hinze, S. Volkwein, Proper orthogonal decomposition surrogate models for nonlinear dynamical systems: error estimates and suboptimal control, Lect. Notes Comput. Sci. Eng. 45 (2005) 261–306.
[38] M. Gunzburger, J. Peterson, J. Shadid, Reduced-order modeling of time-dependent PDEs with multiple parameters in the boundary data, Comput. Methods Appl. Mech. Eng. 196 (2007) 1030–1047.
[39] T. Bui-Thanh, K. Willcox, O. Ghattas, B. van Bloemen Waanders, Goal-oriented, model-constrained optimization for reduction of large-scale systems, J. Comput. Phys. 224 (2) (2007) 880–896.
[40] S. Sen, Reduced basis approximation and a posteriori error estimation for many-parameter heat conduction problems, Numer. Heat Transf., Part B: Fundamentals (submitted for publication).
[41] rbMIT Software: http://augustine .mit.edu/methodology/methodology_rbMIT_System.htm, ©MIT, Cambridge, MA, 2007.
[42] A.T. Patera, G. Rozza, Reduced Basis Approximation and a Posteriori Error Estimation for Parametrized PDEs, MIT-Pappalardo Graduate Monographs in Mechanical Engineering Series (in press).